

ISTANBUL TECHNICAL UNIVERSITY ★ GRADUATE SCHOOL OF SCIENCE
ENGINEERING AND TECHNOLOGY

**EFFECT OF SECOND ORDER VELOCITY SLIP AND TEMPERATURE JUMP
BOUNDARY CONDITIONS ON ENTROPY GENERATION OF A FLOW
OVER ROTATING DISK IN CASE OF BLOWING AND SUCTION**

M.Sc. THESIS

Ahmet Yaşar GÜNEŞ

**Department of Aeronautics and Astronautics Engineering
Aeronautics and Astronautics Engineering Master Programme**

JANUARY 2013

ISTANBUL TECHNICAL UNIVERSITY ★ GRADUATE SCHOOL OF SCIENCE
ENGINEERING AND TECHNOLOGY

**EFFECT OF SECOND ORDER VELOCITY SLIP AND TEMPERATURE JUMP
BOUNDARY CONDITIONS ON ENTROPY GENERATION OF A FLOW
OVER ROTATING DISK IN CASE OF BLOWING AND SUCTION**

M.Sc. THESIS

Ahmet Yaşar GÜNEŞ
(511051031)

Department of Aeronautics and Astronautics Engineering
Aeronautics and Astronautics Engineering Master Programme

Thesis Advisor: Prof. Dr. İbrahim ÖZKOL

JANUARY 2013

İSTANBUL TEKNİK ÜNİVERSİTESİ ★ FEN BİLİMLERİ ENSTİTÜSÜ

**ÜFLEME VE EMME KOŞULLARI ALTINDA İKİNCİ DERECE HIZ
KAYMASI VE SICAKLIK SIÇRAMASI SINIR ŞARTLARININ DÖNEN
DİSK ÜZERİNDEKİ AKIŞTAKİ ENTROPİ ÜRETİMİNE ETKİSİ**

YÜKSEK LİSANS TEZİ

**Ahmet Yaşar GÜNEŞ
(511051031)**

Uçak ve Uzay Mühendisliği Anabilim Dalı

Uçak ve Uzay Mühendisliği Programı

Tez Danışmanı: Prof. Dr. İbrahim ÖZKOL

OCAK 2013

Ahmet Yaşar Güneş , a **M.Sc.** student of ITU **Graduate School of Science Engineering and Technology** student ID 511051031, successfully defended the thesis “**Effect Of Second Order Velocity Slip And Temperature Jump Boundary Conditions On Entropy Generation Of A Flow Over Rotating Disk In Case Of Blowing And Suction**”, which he/she prepared after fulfilling the requirements specified in the associated legislations. before the jury whose signatures are below.

Thesis Advisor : **Prof. Dr. İbrahim ÖZKOL**

İstanbul Technical University

Jury Members : **Prof. Dr. Metin Orhan KAYA**

İstanbul Technical University

Prof. Dr. Erol UZAL

İstanbul University

FOREWORD

Foremost, I would like to express my sincere gratitude to my advisor Prof. Dr. İbrahim ÖZKOL for the continuous support of my study and research, for his patience, motivation, enthusiasm, and immense knowledge. His guidance helped me in all the time of research and writing of this thesis. I would also like to thank Asst. Prof. Güven KÖMÜRĞÖZ and Dr. Aytaç ARIKOGLU for all their supports.

Besides my advisor, I would like to thank the rest of my jury members: Prof. Dr. Metin Orhan KAYA and Prof. Dr. Erol UZAL for their encouragement and insightful comments.

I would like to thank my parents Sebahat GÜNEŞ and Recai GÜNEŞ for supporting me spiritually throughout my life.

Especially, I would like to give my special thanks to my wife Demet GÜNEŞ whose patient love enabled me to complete this work.

January 2013

Ahmet Yaşar GÜNEŞ
Astronautics Engineer

TABLE OF CONTENTS

	<u>Page</u>
TABLE OF CONTENTS.....	ix
SUMMARY	xix
1. INTRODUCTION.....	1
1.1 Literature Review	1
1.2 Research Objectvives and Goals	3
2. THEORITICAL CONSIDERATION.....	5
2.1 Fluid Modelling and Flow Regimes	5
2.2 Flow Over Rotating Disk	8
2.2.1 Flow Field	8
2.2.2 Thermal Field	9
2.3 Velocity Slip and Temperature Jump.....	10
2.4 Entropy Generation	12
3. DIFFERENTIAL TRANSFORM METHOD	13
3.1 Theorems	13
4. ANALYSIS AND SOLUTION OF EQUATIONS	15
4.1 Transform of The Equations	15
4.1.1 Flow Field	15
4.1.2 Thermal Field	16
4.1.3 Entropy Generation	17
4.2 Solution of The Equations.....	19
5. EFFECT OF SECOND ORDER VELOCITY SLIP AND TEMPERATURE JUMP CONDITIONS ON ROTATING DISK FLOW IN CASE OF BLOWING AND SUCTION WITH ENTROPY GENERATION.....	23
5.1 Flow Field	23
5.2 Thermal Field	40
5.3 Entropy Generation	45
6. CONCLUSION.....	47
REFERENCES.....	49
CURRICULUM VITA	53

LIST OF TABLES

	<u>Page</u>
Table 2.1: Thermophysical properties of typical gases used in microdomain applications at atmospheric conditions (298 K and 1 atm).....	6
Table 2.2: Thermal and tangential momentum accommodation coefficients for typical gases and surfaces.	11

LIST OF FIGURES

	<u>Page</u>
Figure 2.1 : Fluid Modelling	5
Figure 2.2 : Classifications of the gas flow regimes and governing equations over the range of Knudsen Numbers	7
Figure 2.3 : Typical MEMS and nanotechnology applications in standart atmospheric conditions span the entire Knudsen regime.....	7
Figure 2.4 : Coordinate system for the rotating disk flow	8
Figure 5.1 : Variation of $F(\zeta)$ with respect to ζ for first order and second order slip. Difference between first and second order value of $F(\zeta)$ with respect to ζ	24
Figure 5.2 : Variation of $G(\zeta)$ with respect to ζ for first and second order slip. Difference between first and second order value of $G(\zeta)$ with respect to ζ	25
Figure 5.3 : Variation of $H(\zeta)$ with respect to ζ for first and second order slip. Difference between first and second order value of $H(\zeta)$ with respect to ζ	26
Figure 5.4 : Variation of $\theta(\zeta)$ with respect to ζ for first order and second order slip. Difference between first and second order value of $\theta(\zeta)$ with respect to ζ	27
Figure 5.5 : Variation of $\theta(\zeta)$ with respect to ζ for first order and second order slip in Neutral case ($W=0$). Difference between first and second order value of $\theta(\zeta)$ with respect to ζ	28
Figure 5.6 : Variation of $\theta(\zeta)$ with respect to ζ for first order and second order slip in Suction case ($W=-1$). Difference between first and second order value of $\theta(\zeta)$ with respect to ζ	29
Figure 5.7 : Variation of $\theta(\zeta)$ with respect to ζ for first order and second order slip in Blowing case ($W=1$). Difference between first and second order value of $\theta(\zeta)$ with respect to ζ	30
Figure 5.8 : Variation of N_g with respect to slip factor and jump factor ($\bar{r}=1$) in Neutral case ($W=0$).....	31
Figure 5.9 : Variation of N_g with respect to slip factor and jump factor ($\bar{r}=1$) in Suction case ($W=-1$)	32
Figure 5.10 : Variation of N_g with respect to slip factor and jump factor ($\bar{r}=1$) in Blowing case ($W=1$)	33
Figure 5.11 : Variation of $N_{g,av}$ with respect to slip factor and jump factor for first and second order in Neutral case ($W=0$)	34
Figure 5.12 : Variation of $N_{g,av}$ with respect to slip factor and jump factor for first and second order in Suction case ($W=-1$).....	35
Figure 5.13 : Variation of $N_{g,av}$ with respect to slip factor and jump factor for first and second order in Blowing case ($W=1$)	36
Figure 5.14 : Variation of N_g with respect to \bar{r} and ζ in Neutral case ($W=0$).....	37
Figure 5.15 : Variation of N_g with respect to \bar{r} and ζ in Suction case ($W=-1$).....	38
Figure 5.16 : Variation of N_g with respect to \bar{r} and ζ in Blowing case ($W=1$).....	39

Figure 5.17 : Variation of Be with respect to slip factor and jump factor ($\bar{r}=1$) in Neutral case ($W=0$)	40
Figure 5.18 : Variation of Be with respect to slip factor and jump factor ($\bar{r}=1$) in Suction case ($W=-1$)	41
Figure 5.19 : Variation of Be with respect to slip factor and jump factor ($\bar{r}=1$) in Blowing case ($W=1$)	42
Figure 5.20 : Variation of Be with respect to \bar{r} and ζ in Neutral case ($W=0$)	43
Figure 5.21 : Variation of Be with respect to \bar{r} and ζ in Suction case ($W=-1$)	44
Figure 5.22 : Variation of Be with respect to \bar{r} and ζ in Blowing case ($W=1$)	45

LIST OF SYMBOLS

Be	Bejan number, N_H / N_g
Be _{av}	average Bejan number
Br	rotational Brinkman number, $\mu\Omega^2 R^2 / k\Delta T$
c _p	constant temperature specific heat, $\text{kJ kg}^{-1} \text{K}^{-1}$
Ec	Eckert number, $(\Omega R)^2 / c_p \Delta T$
F, f	dimensionless radial velocities
G, g	dimensionless circumferential velocities
H, h	dimensionless axial velocity
\tilde{F}	differential transform of f
\tilde{G}	differential transform of g
\tilde{H}	differential transform of h
k	thermal conductivity, $\text{W m}^{-1} \text{K}^{-1}$
Kn	Knudsen number, λ / R
n	number of terms considered in DTM calculation
N _g	dimensionless entropy generation rate, $\dot{S}_G'' / (k\Omega\rho\Delta T / \mu T_w)$
N _{g,av}	average entropy generation rate
N _H	entropy generation due to heat transfer irreversibility
N _F	entropy generation due to fluid friction irreversibility
p	pressure, N/m^2
P	dimensionless pressure
Pr	Prandtl number, $\mu c_p / k$
r	radial coordinate, m
\bar{r}	dimensionless radial coordinate, $\bar{r} = r / R$
R,	radius of the disk, m

Re	rotational Reynolds number, $Re = \Omega R^2 / \nu$
\dot{S}_G	entropy generation rate
T	temperature, K
T_w	temperature on the disk, K
T_s	slip temperature, K
T_∞	temperature at infinity, K
u	radial velocity, m/s
U_s	slip flow velocity, m/s
U_w	velocity of the disk, m/s
v	circumferential velocity, m/s
w	axial velocity, m/s
z	axial coordinate, m
W	uniform suction or blowing parameter

Greek Letters

α	dimensionless temperature difference, $\alpha = \Delta T / T_w$
β	specific heat ratio
γ	slip factor
η	jump factor
β_{v1}	first order velocity slip factor
β_{v2}	second order velocity slip factor
β_{t1}	first order thermal jump factor
β_{t2}	second order thermal jump factor
ΔT	temperature difference, $T_w - T_\infty$
ζ	dimensionless axial coordinate, $z\sqrt{\Omega/\nu}$
θ	dimensionless temperature, $\theta = (T - T_\infty) / (T_w - T_\infty)$
λ	mean free path, m
μ	dynamic viscosity, $Nm^{-2}s$

ν	kinematic viscosity, m ² /s
ξ	stretched dimensionless axial coordinate, $e^{-c\xi}$
ρ	density, kg/m ³
σ_v	tangential momentum accommodation coefficient
σ_t	energy accommodation coefficient
dE_i	energy fluxes of incoming molecules per unit time
dE_r	energy fluxes of reflected molecules per unit time
dE_r	energy fluxes of reflected molecules per unit time
τ_i	tangential momentum of incoming molecules
τ_r	tangential momentum of reflected molecules
τ_w	tangential momentum of reemitted molecules
ϕ	generalized thermal jump factor
Ψ	group parameter, $\Psi = Br / \alpha Re^2$
Ω	angular velocity of the rotating disk, rad/s
∇	dimensionless volume

EFFECT OF SECOND ORDER VELOCITY SLIP AND TEMPERATURE JUMP BOUNDARY CONDITIONS ON ENTROPY GENERATION OF A FLOW OVER ROTATING DISK IN CASE OF BLOWING AND SUCTION

SUMMARY

In this study, the effect of second order velocity slip and temperature jump boundary conditions on entropy generation of a flow over rotating disk in case of blowing and suction cases is investigated. As a model, the flow over a rotating single free disk for steady and axially symmetrical case in a Newtonian ambient fluid is chosen. The classical approach, which is introduced by Von Karman, is used with transformations introduced by Benton to reduce non-linear flow and thermal field equations to ordinary differential equations. Then flow field equations are solved by using differential transform method (DTM) and thermal field equations solved by numerical integration.

The flow field, which is consisted of radial, circumferential and axial velocity components, is plotted separately. Velocity slip effects in both first order and second order boundary conditions are monitored. In comparison with no-slip flow regime, radial and circumferential velocities adjacent disk surface are different from disk velocity. Slip boundary conditions reduce the radial, circumferential and axial velocity gradients away from disk surface. Second order effects become significant on radial and axial velocities.

The thermal field under the condition that heat transfer is only axial direction is plotted. The thermal field is graphed in blowing, suction and neutral case. First and second order velocity slip and temperature jump effects are observed case by case. The paramount difference between first and second order boundary conditions occur in blowing case. The first and second order effects are closer in suction and neutral case.

Entropy generation equations for this system is then derived and non-dimensionalized. These equations interpreted for various physical cases by using non-dimensional parameters of fluid and thermal fields in blowing and suction case. The local entropy generation and average entropy generation rates with first and second order boundary conditions are plotted. Additionally Bejan numbers, which are the ratio of entropy generation due to heat transfer to the total entropy generation, are monitored. It is observed that the effect of second order boundary conditions is to reduce velocity and temperature gradient so the magnitude of entropy generation is decrease.

ÜFLEME VE EMME KOŞULLARI ALTINDA İKİNCİ DERECE HIZ KAYMASI VE SICAKLIK SIÇRAMASI SINIR ŞARTLARININ DÖNEN DİSK ÜZERİNDEKİ AKIŞTAKİ ENTROPİ ÜRETİMİNE ETKİSİ

ÖZET

Bu çalışmada ikinci derece hız kayması ve sıcaklık sıçraması sınır şartlarının, dönen disk üzerindeki akışın, emme ve üfleme koşulları altındaki entropi üretimine etkisi incelenmiştir. Model olarak, basit dönen disk üzerinde istikrarlı, eksenel olarak simetrik Newtonian akış seçilmiştir. Von Karman tarafından geliştirilen klasik yaklaşımda, Benton dönüşümleri kullanılarak, lineer olmayan akış ve termal alan denklemleri adi diferansiyel denklemlere indirgenmiştir. Sonra akış alanı denklemleri diferansiyel dönüşüm metodu (DTM) yardımıyla, termal alan denklemleri ise nümerik integral yöntemi ile çözülmüştür.

Bu çalışmada akış rejimlerini belirlemede etkin olan Knudsen sayısı (Kn) hakkında bilgi verilmiştir ve Knudsen sayısına bağlı olarak akış rejimleri anlatılmıştır. Bu rejimlerdeki uygulama alanlarından örnekler verilmiştir. Hangi rejimlerde hangi denklemlerin ve sınır şartlarının kullanılmasının uygun olduğu hakkında özet bilgiler verilmiştir. Bu kaymasız ve kaymalı akış rejimlerinde, hız kayması ve sıcaklık sıçraması sınır şartları altında geçerlidir.

Birinci ve ikinci derece sınır şartları detaylı olarak anlatılmıştır. Kayma sınır şartlarını oluşturan parametreler hakkında bilgi verilmiş ve bu parametrelerden bazıları hakkında daha önce yapılan deneysel sonuçlar tablolar halinde listelenmiştir. Hız kaymasına etki eden parametreler, hız kayma parametresi olarak ele alınmış ve denklemler kayma parametresinin farklı değerlerine göre çözülmüştür. Aynı şekilde sıcaklık sıçramasına etki eden parametreler sıcaklık sıçrama parametresi olarak ele alınmıştır. Termal alana hem hız kayması hem de sıcaklık sıçraması sınır şartları etki ettiğinden. Bu parametrelere bağlı olarak ayrı ayrı termal grafikler çizilmiştir.

Radyal, çevresel ve eksenel hız bileşenlerinin oluşturduğu akış alanı incelenmiş ve grafikleri ayrı ayrı çizilmiştir. Çizilen grafiklerde hem birinci derece hız kayması hem de ikinci derece hız kayması etkileri gösterilmiştir. Birinci derece hız kayması sınır koşulu altında ve ikinci derece hız kayması koşulu altındaki hız profilleri arasındaki farklar da ayrıca çizilmiştir. Kaymasız akış rejiminde diskin hemen üzerindeki akışın hızı ile diskin hızı aynı olmasına rağmen kaymalı akış rejiminde diskin hızı ile diske bitişik akışkanın hızı arasında fark oluşmaktadır. Diskin hemen üzerindeki bu fark sadece radyal ve çevresel hız bileşenlerinde oluşmaktadır. Birinci derece ve ikinci derece sınır koşulları hız alanı çözüldüğünde en büyük farkın radyal ve eksenel hız bileşenlerinde olduğu görülmüştür. Çevresel hız bileşeninde ikinci derece sınır şartı etkisi ihmal edilecek kadar az olduğu tespit edilmiştir.

Isı transferinin sadece eksenel yönde olduğu varsayılarak, termal alan denlemleri çözülmüştür. Emme, üfleme ve nötr koşullar altındaki boyutsuz sıcaklık değişimi grafikleri çizilmiştir ve etkileri incelenmiştir. Emme, üfleme ve nötr şartlarda birinci ve ikinci derece hız kayması, birinci ve ikinci derece sıcaklık sıçraması sınır şartları ayrı ayrı uygulanmış ve oluşan sonuçlar incelenmiştir.

Isı transferinin sadece eksenel yönde değişimi varsayıldığından sadece eksenel yöndeki hız bileşeninin sıcaklık dağılımına etkisi olduğu belirtilmiştir. Kaymaz akış rejiminde disk yüzeyinin sıcaklığı ile diskin hemen üzerindeki akışkanın sıcaklığı aynı olmasına rağmen, hız kayması ve sıcaklık sıçraması sınır şartlarının etkili olduğu kaymalı akış rejiminde disk yüzeyinin sıcaklığı ile diskin hemen üzerindeki akışkanın sıcaklığı arasında fark gözlenmiştir. Bu fark temelde sıcaklık sıçrama sınır şartına bağlı olduğu görülmüştür. Hız kayma ve sıcaklık sıçrama parametrelerinin artması durumunda diskin üzerindeki akışkanın sıcaklık dağılım gradyanının azaldığı görülmüştür. Sıcaklık dağılımları emme, üfleme ve nötr şartlarda incelenmiş ve birinci ile ikinci derece sınır şartları arasındaki en büyük farkın üfleme şartında olduğu tespit edilmiştir.

Bu sistem için entropi üretimi denklemleri elde edilmiş ve boyutsuz hale getirilmiştir. Bu denklemler emme ve üfleme koşullarında, boyutsuz akış ve sıcaklık alanı parametreleri kullanılarak yorumlanmıştır.

Yerel entropi üretim oranları hesaplanıp, grafiksel olarak gösterilmiştir. Bu grafiklerde birinci ve ikinci derece hız kayma parametresinin etkilerinin yanında birinci ve ikinci derece sıcaklık sıçrama parametrelerinin etkileri de ayrı ayrı gösterilmiştir. Ayrıca hem radyal hem de eksenel yöndeki local entropi üretim oranları üç boyutlu halde çizilmiştir. En yüksek entropi üretim oranı disk yüzeyine ve diskin merkezinden uzakta gözlemlenmektedir. Artan hız kayma ve sıcaklık sıçrama parametreleri yerel entropi oranını azaltmakta olduğu belirlenmiştir. Üfleme durumunda birinci derece sınır koşulları ile ikinci derece sınır koşulları arasındaki farkın, emme ve nötr durumlarına göre daha fazla olduğu gözlenmiştir.

Benzer bir şekilde ortalama entropi üretim oranları da hesaplanıp, grafiksel olarak gösterilmiştir. Bu grafiklerde hem emme, üfleme ve nötr şartlar gözönünde bulundurularak hem de birinci ve ikinci derece sınır şartları dikkate alınarak ayrı ayrı gösterilmiştir. Hız kayma ve sıcaklık sıçrama parametreleri arttıkça ortalama entropi üretim oranları azalmaktadır. Üfleme koşullarında ikinci derece sınır şartlarının etkileri emme ve nötr duruma göre daha belirgin hale gelmektedir.

Isı transferinden oluşan entropi üretiminin toplam entropi üretimine oranını temsil eden Bejan sayısı (Be), emme, üfleme ve nötr şartlarda incelenmiştir. Hem birinci derece ve ikinci derece hız kayma sınır şartları hem de birinci ve ikinci derece sıcaklık sıçraması sınır şartlarının etkileri belirlenip grafiksel olarak gösterilmiştir. Buna ek olarak Bejan sayısının radyal ve eksenel yöndeki dağılımları emme, üfleme ve nötr şartlarda incelenmiştir. Bunun yanında birinci ve ikinci derece sınır şartı etkilerinin radyal ve eksenel yöndeki dağılımları çizilmiştir. Hız kayma parametresi arttıkça Bejan sayısı artmaktadır yani ısı transferinden oluşan entropi üretiminin toplam entropi üretimine oranının artmakta olduğu gözlenmiştir. Bunun aksine sıcaklık sıçrama parametresi arttıkça Bejan sayısı azalmaktadır yani ısı transferinden oluşan entropi üretiminin toplam entropi üretimine oranının azalmakta olduğu görülmüştür.

Hız kayma ve sıcaklık sıçrama parametreleri arttıkça hız ve sıcaklık gradyanleri azaldığından entropi üretim oranlarında da azalma görülmektedir. Entropi üretim oranı, disk yüzeyi üzerinde ve boyutsuz disk yarıçapının 1 olduğu bölgede en yüksek değerini almaktadır. Ayrıca Bejan sayısı diskin merkezinde en fazla değer ulaşırken, radyal yönde gittikçe azalma görülmektedir.

1. INTRODUCTION

It is required to know how efficiently have we used today's energy sources and the efficiency of our energy transformation systems. During the process of energy transformation, the contributions of the irreversible agents should be known. We have all noticed that there is a strong connection between energy usage and economic growth. We should be kept in mind that nothing happens; nothing is created, without the irreversible dissipation of high-grade energy into degraded or less useable.

1.1 Literature Review

Flow over a rotating disk is of great interest in industrial, geothermal, geophysical, technological and engineering practices such as gas turbine design, electronic components having rotary parts, computer disk drives, estimating the flight path of rotating wheels and spin-stabilized missiles and modeling of many geophysical vortices. Von Karman [1] created a milestone in this problem. He defined the Navier-Stokes equations governing the Newtonian flow over the rotating disk flow, reduced to a self-similar form and he obtained an approximate solution. Cochran [2] derived a more accurate solution to the same problem.

Studies on rotating disk flow and heat transfer have been subjected to considerable interest from day to day. Attia investigated the steady laminar flow of a viscous incompressible fluid due to the rotating of a disk of infinite extent in a porous medium [3]. The laminar flow of a Newtonian bulk fluid arising from a solid rotating disk lubricated by a non-Newtonian liquid film is studied by Andersson [4].

Osalusi et al. studied the laminar convective and slip flow of an electrically conducting Newtonian fluid with variable properties over a rotating porous disk [5,6]. The study of laminar flow and heat transfer generated by two infinite parallel disks separated by a gas-filled micro-gap was considered by Jiji [7]. In another study, new three-dimensional solutions of the Navier–Stokes equations governing the steady-state stationary viscous flow of electrically conducting fluid associated with a

single rotating disk is proposed by Turkyilmazoglu [8]. Ozkol et al. determined the effect of slip on entropy generation in a single rotating disk in MHD flow [9].

On the other hand, there have been various researches on micro fluidic systems for compact reactor technologies in recent years [10]. Micro-Flow devices (MFD), which are substantially used in complex systems for medical diagnosis and surgery, chemical analysis, biotechnology, electronic cooling, are actually downscaled devices; such as micro-channels, mixers, pumps, and heat pipes [11]. Heat and fluid flow characteristics through micro devices are different from the macro scale counterparts. Velocity slip and temperature jump are constitute this difference substantially.

The slip flow regime has been widely studied and these studies increasingly continue. Navier-Stokes and energy equations with slip boundary conditions are valid in the slip flow regime. Velocity slip and temperature jump are the two major parameter of slip BCs. Velocity slip is very important for precise analysis of the behavior of micro flows. On the other hand, temperature jump has become significant to determine the heat transfer in this type flow regime. Aziz [12] considered the effect of slip flow on the thermal boundary layer over a flat plate with a constant heat flux boundary condition instead of a constant temperature boundary condition. Ozkol et.al. [13] analyzed the combined effects of velocity and temperature jump on the entropy generation over a rotating disk. Renksizbulut et al. studied incompressible gas flows and heat transfer in rectangular micro channels of various aspect ratios [14]. In their study, they carried out for various Knudsen numbers related to the slip-flow regime by using three-dimensional Navier-Stokes and energy equations together with velocity-slip and temperature-jump boundary conditions.

The second order temperature jump and velocity slip condition effects were investigated in other studies. Ameen et al. studied micro tube gas flows with second-order velocity slip and temperature jump boundary conditions [15]. He investigated heat transfer in the slip regime for fully developed flow in circular microtubes. Meolans studied thermal slip boundary conditions in vibrational nonequilibrium flows [16]. Karniadakis and Beskok [11] proposed a general, second order slip condition in nondimensional form and provided a comparison of the various forms of the slip regime boundary conditions. In another studies of authors, the fundamental

laws and the methodology of gas microflows, i.e., gas flows in devices with characteristic dimensions of the order of a micron were studied [17]. Deissler's [18] second-order model was proposed relatively recently to compare to the other slip models. Hamdan [19] studied the effects of adding the second-order term to the velocity-slip and temperature-jump boundary condition on the solution of four cases of basic gas micro-flow problems, the transient Couette flow, the pulsating Poiseuille flow, the Stoke's second problem flow and the transient natural convection flow, studied by Haddad et al. [20]. Hooman [21] presented the closed form solutions for local and bulk temperature distribution as well as the Nusselt number in the fully developed region and extends the analysis to the Second Law where local and average values of the entropy generation and the Bejan number are reported in his study. The aim of Niazmand's study [22] is to determine the high order slip and thermal creep effects in micro channel natural convection. Zahmatkesh et al. [23] focused on the derivation of new velocity-slip and temperature-jump boundary conditions for rarefied non-reacting gas mixtures.

Differential Transform Method (DTM) is semi-numerical–analytical technique that formulizes Taylor series in a very different manner. Zhou [24] introduced DTM in a study about electrical circuits. Mao [25] designed a piezoelectric modal sensor for non-uniform Euler-Bernoulli beams with rectangular cross-section by using differential transformation method. Rahimi et al. [26] used DTM for temperature distribution in a radiating fin. Ozkol and Arikoglu [27] successfully extended DTM, by presenting and proving new theorems, to the solution of differential-difference equations.

1.2 Research Objectives and Goals

In this study, the combined effects of the velocity slip and temperature jump on the thermal and flow fields are investigated in detail for different values of the non-dimensional field parameters for a rotating disk. Differential Transform Method (DTM) is employed to solve the reduced governing equations under the assumptions of velocity and thermal jump conditions on the disk surface. In order to show the second order temperature jump and velocity slip condition effects on the rotating disk type flow three different flow field cases are considered, i.e., neutral, suction

and blowing. To evaluate the efficiency of such rotating fluidic system, the entropy generation equation is derived and non-dimensionalized. Additionally, special attention has been given to Bejan (Be) and Entropy generation numbers, their characteristics and their dependency on various parameters, i.e., slip and jump factors. First and second order slips and jump boundary conditions are applied separately and their sole effects are shown. Differences in applying first and second order slip and jump boundary conditions are depicted.

Graphical representations for local and volumetric values of entropy generation and Be number are presented for different values of the flow parameters.

2. THEORETICAL CONSIDERATION

2.1 Fluid Modelling and Flow Regimes

There are generally two ways of modeling a flow field such as molecular model and continuum model. Molecular method consists of deterministic and probabilistic methods. In the continuum method, the velocity, density, pressure, temperature is defined at every point in space and time. Fluid modeling illustrated in Fig.2.1

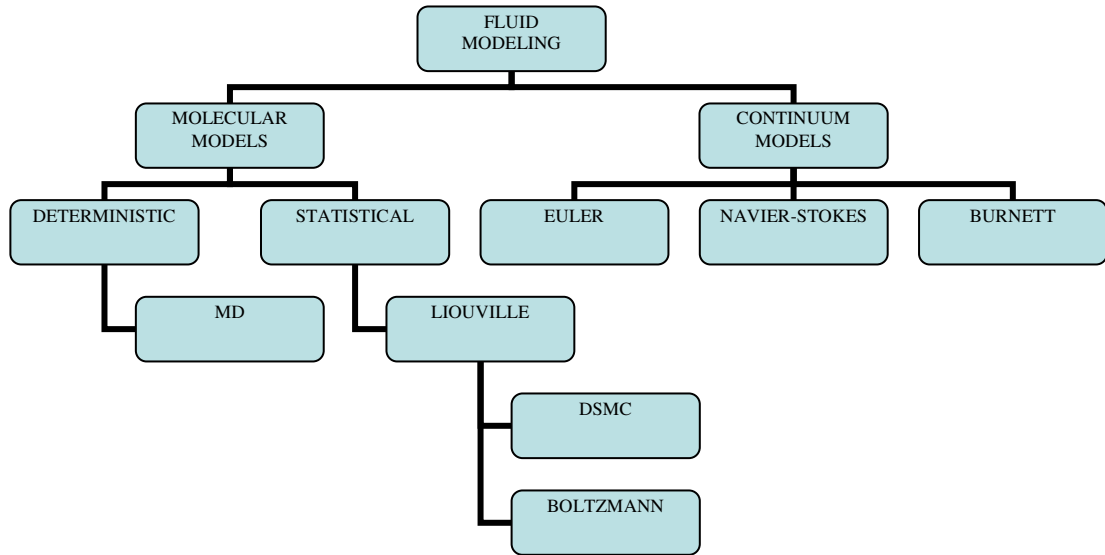


Figure 2.1 : Fluid Modelling

Microscale fluid system behaves differently than macroscale fluid systems. Flow characteristic change as per fluid regimes. Most important parameter is rarefaction, which is represented by Knudsen Number (Kn). [11]

$$Kn = \frac{\lambda}{L} = \sqrt{\frac{\pi\beta}{2}} \frac{Ma}{Re} \quad (2.1)$$

Where λ is mean free path, β is specific heat ratio, Ma is mach number and Re is Reynolds number. Thermophysical properties of typical gases used in microdomain applications listed in Table 2.1.

Table 2.1: Thermophysical properties of typical gases used in microdomain applications at atmospheric conditions (298 K and 1 atm)

Gas	Density [kg/m ³]	Dynamic Viscosity [kg/(m s)]	Thermal Con- ductivity [W/(m K)]	Thermal Diffusivity [m ² /s]	Specific Heat [J/(kg K)]	Mean Free Path [m]
Air	1.293	1.85E-5	0.0261	2.01E-5	1004.5	6.111E-8
N ₂	1.251	1.80E-5	0.0260	2.00E-5	1038.3	6.044E-8
CO ₂	1.965	1.50E-5	0.0166	1.00E-5	845.7	4.019E-8
O ₂	1.429	2.07E-5	0.0267	2.04E-5	916.9	6.503E-8
He	0.179	1.99E-5	0.150	1.60E-4	5233.5	17.651E-8
Ar	1.783	2.29E-5	0.0177	1.93E-5	515.0	6.441E-8

Effects of rarefaction become more important when the Knudsen number increases and thus pressure drop, shear stress, heat flux, and corresponding mass flow rate cannot be estimated from flow and heat transfer models based on the continuum hypothesis. Flow regimes divided into four regimes according to Knudsen Numbers as follows; [30]

For $Kn \leq 0.01$ (the continuum flow regime) conventional continuum conservation of Momentum and energy methods, such as the Navier-Stokes equations with no-slip boundary condition, may be used.

For $0.01 \leq Kn \leq 0.1$ (the slip flow regime) Navier-Stokes equations may be used with velocity slip and temperature jump boundary conditions

For $0.1 \leq Kn \leq 10$ (the transition regime) Both numerical solution of Boltzmann equation and Direct Simulation Monte Carlo method may be used

For $Kn > 10$ (the free molecular regime) Either Lattice Boltzmann equation or DSMC methods are commonly used.

These flow regimes is very important in order to choose the methods used for the modeling and estimation of the microflows. Fig.2.2 illustrates different regimes and equations of the microflow depending on the Knudsen Number.[33]

The operation regimes of typical microsystems at standard temperature and pressure are shown in Fig.2.3 Micro Electro-Mechanical System (MEMS) devices operate in a wide range of flow regimes covering the continuum, slip, and transition flow. [11]

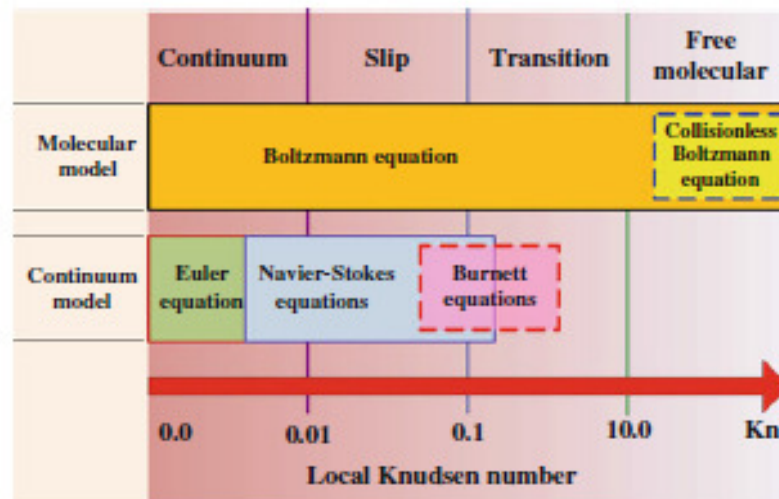


Figure 2.2 : Classifications of the gas flow regimes and governing equations over the range of Knudsen Numbers (Beskok, 2002)

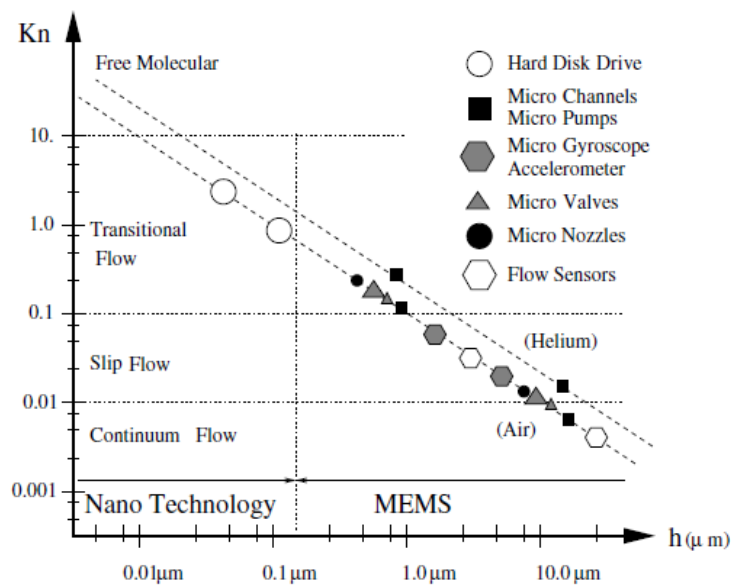


Figure 2.3 : Typical MEMS and nanotechnology applications in standard atmospheric conditions span the entire Knudsen regime. (Beskok,2002)

2.2 Flow Over Rotating Disk

The flow over rotating disk is modelled in a cylindrical coordinate system as an infinite planar disk. The fluid is assumed to be incompressible with constant properties. A schematic diagram of the problem illustrated in Fig. 2.4

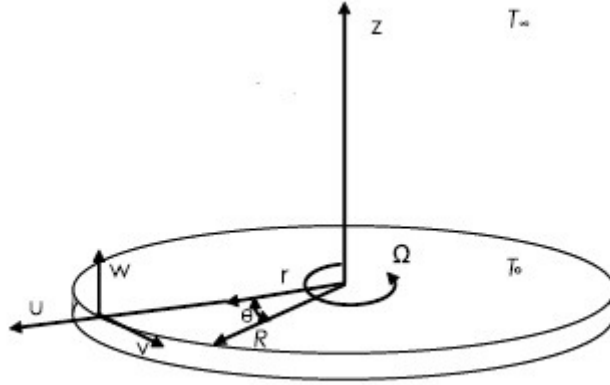


Figure 2.4 : Coordinate system for the rotating disk flow

2.2.1 Flow Field

An incompressible flow over rotating disk described with the Navier-Stokes equations, which are four coupled nonlinear partial differential equations for four unknown functions, which are the three components of u and the pressure p , in a Cartesian coordinate system shown as follow. [30]

$$\frac{\partial u_1}{\partial t} + u_1 \frac{\partial u_1}{\partial x} + u_2 \frac{\partial u_1}{\partial y} + u_3 \frac{\partial u_1}{\partial z} + \frac{1}{\rho} \frac{\partial p}{\partial x} = \frac{\mu}{\rho} \left(\frac{\partial^2 u_1}{\partial x^2} + \frac{\partial^2 u_1}{\partial y^2} + \frac{\partial^2 u_1}{\partial z^2} \right) \quad (2.1)$$

$$\frac{\partial u_2}{\partial t} + u_1 \frac{\partial u_2}{\partial x} + u_2 \frac{\partial u_2}{\partial y} + u_3 \frac{\partial u_2}{\partial z} + \frac{1}{\rho} \frac{\partial p}{\partial y} = \frac{\mu}{\rho} \left(\frac{\partial^2 u_2}{\partial x^2} + \frac{\partial^2 u_2}{\partial y^2} + \frac{\partial^2 u_2}{\partial z^2} \right) \quad (2.3)$$

$$\frac{\partial u_3}{\partial t} + u_1 \frac{\partial u_3}{\partial x} + u_2 \frac{\partial u_3}{\partial y} + u_3 \frac{\partial u_3}{\partial z} + \frac{1}{\rho} \frac{\partial p}{\partial z} = \frac{\mu}{\rho} \left(\frac{\partial^2 u_3}{\partial x^2} + \frac{\partial^2 u_3}{\partial y^2} + \frac{\partial^2 u_3}{\partial z^2} \right) \quad (2.4)$$

$$\frac{\partial u_1}{\partial x} + \frac{\partial u_2}{\partial y} + \frac{\partial u_3}{\partial z} = 0 \quad (2.5)$$

$\rho(X,t)$ is the fluid density, $u(X,t)$ is the velocity vector field and $p(X,t)$ is the pressure;

$X \in R^{3d}$ is the spatial coordinate. μ is the dynamic viscosity.

Consider the steady, incompressible flow over a single free disk in a Newtonian fluid. The equations of steady motion in the cylindrical coordinates (r,θ,z) are given as follows;

$$u \frac{\partial u}{\partial r} + w \frac{\partial u}{\partial z} - \frac{v^2}{r} + \frac{1}{\rho} \frac{\partial p}{\partial r} = \frac{\mu}{\rho} \left(\frac{\partial^2 u}{\partial r^2} + \frac{1}{r} \frac{\partial u}{\partial r} - \frac{u}{r^2} + \frac{\partial^2 u}{\partial z^2} \right) \quad (2.6)$$

$$u \frac{\partial v}{\partial r} + w \frac{\partial v}{\partial z} + \frac{uv}{r} = \frac{\mu}{\rho} \left(\frac{\partial^2 v}{\partial r^2} + \frac{1}{r} \frac{\partial v}{\partial r} - \frac{v}{r^2} + \frac{\partial^2 v}{\partial z^2} \right) \quad (2.7)$$

$$u \frac{\partial w}{\partial r} + w \frac{\partial w}{\partial z} + \frac{1}{\rho} \frac{\partial p}{\partial z} = \frac{\mu}{\rho} \left(\frac{\partial^2 w}{\partial r^2} + \frac{1}{r} \frac{\partial w}{\partial r} + \frac{\partial^2 w}{\partial z^2} \right) \quad (2.8)$$

$$\frac{\partial(ru)}{\partial r} + \frac{\partial(rw)}{\partial z} = 0 \quad (2.9)$$

Where u is the radial, v is the circumferential and w is the axial components of the velocity.

2.2.2 Thermal Field

After neglecting dissipation terms, the energy equation can be written as follows;

$$\rho c_p \left(u \frac{\partial T}{\partial r} + w \frac{\partial T}{\partial z} \right) - k \left(\frac{\partial^2 T}{\partial z^2} + \frac{\partial^2 T}{\partial r^2} + \frac{1}{r} \frac{\partial T}{\partial r} \right) = 0 \quad (2.10)$$

Where T is the temperature, k is the thermal conductivity, c_p is the constant temperature specific heat. It is assumed that heat transfer is only in the z direction and then equation (2.10) becomes;

$$\rho c_p \left(w \frac{dT}{dz} \right) - k \frac{d^2 T}{dz^2} = 0 \quad (2.11)$$

2.3 Velocity Slip and Temperature Jump

Microscale fluid system behaves differently than macroscale fluid system because of various factors. For microscale system, rarefaction effects may be considerable. Rarefaction effects become significant while the mean free path of the fluid molecules comparable with the characteristic length of the system rarefaction effects become significant. When this occurs, noncontinuum behaviors begin to develop. While in the slip flow regime ($0.01 \leq Kn \leq 0.1$) continuum equations may be used with velocity slip and temperature jump boundary conditions. In the slip flow regime, boundary conditions named as velocity slip and temperature jump are the state of difference momentum and energy exchange between the fluid molecules and the solid surface. Maxwell and Smoluchowski [11] define first order velocity slip and temperature jump, respectively.

$$U_s - U_w = \frac{2 - \sigma_v}{\sigma_v} \lambda \frac{\partial U_s}{\partial y} + \frac{3}{2\pi} \frac{(\beta - 1)}{\beta} \frac{\lambda^2 \text{Re}}{\text{Ec}} \frac{\partial T}{\partial x} \quad (2.12)$$

$$T_s - T_w = \frac{2 - \sigma_T}{\sigma_T} \left[\frac{2\beta}{\beta + 1} \right] \frac{\lambda}{\text{Pr}} \frac{\partial T}{\partial y} \quad (2.13)$$

Where β is the specific heat ratio, Re is Reynolds number, Ec is Eckert number, Pr is Prandtl number. σ_v and σ_T are tangential momentum and thermal accommodation coefficients, respectively. These accommodation coefficients are defined by;

$$\sigma_T = \frac{dE_i - dE_r}{dE_i - dE_w} \quad (2.14)$$

$$\sigma_v = \frac{\tau_i - \tau_r}{\tau_i - \tau_w} \quad (2.15)$$

Where dE_i and dE_r denote the energy fluxes of incoming and reflected molecules per unit time and dE_w denote the energy flux if all the incoming molecules had been reemitted with the energy flux corresponding to the surface temperature T_w . τ_i and τ_r show the tangential momentum of incoming and reflected molecules, respectively. τ_w is the tangential momentum of reemitted molecules, corresponding

to that of the surface. Some values of thermal and tangential accomodation coefficients for typical gases and surface are tabled in Table 2.2 [11]

Table 2.2: Thermal and tangential momentum accomodation coefficients for typical gases and surfaces. (Beskok, 2002)

Gas	Surface	σ_T	σ_v
Air	Al	0.87–0.97	0.87–0.97
He	Al	0.073	
Air	Iron	0.87–0.96	0.87–0.93
H ₂	Iron	0.31–0.55	
Air	Bronze		0.88–0.95

However, it is possible to solve the Navier-Stokes equations (NS) by applying first order boundary conditions, near transition regime many second order modifications and methods are proposed for accurate solutions. Second order boundary modified conditions proposed by Beskok and Karniadakis [11] shown as follow;

$$U_s - U_w = \frac{2 - \sigma_v}{\sigma_v} \left(\lambda \frac{\partial U_s}{\partial y} + \frac{1}{2} \lambda^2 \frac{\partial^2 U_s}{\partial y^2} \right) \quad (2.16)$$

$$T_s - T_w = \frac{2 - \sigma_T}{\sigma_T} \left[\frac{2\beta}{\beta + 1} \right] \frac{1}{\text{Pr}} \left(\lambda \frac{\partial T}{\partial y} + \frac{\lambda^2}{2} \frac{\partial^2 T}{\partial y^2} \right) \quad (2.17)$$

The concise closed form of second order boundary conditions can be given as below;

$$U_s - U_w = \left(\beta_{v1} \frac{\partial U_s}{\partial y} + \beta_{v2} \frac{\partial^2 U_s}{\partial y^2} \right) \quad (2.18)$$

$$T_s - T_w = \left(\beta_{t1} \frac{\partial T}{\partial y} + \beta_{t2} \frac{\partial^2 T}{\partial y^2} \right) \quad (2.19)$$

Where, β_{v1} and β_{v2} are first and second order velocity slip factors. Similarly, β_{t1} and β_{t2} are first and second thermal jump factors. These factors are introduced respectively.

$$\beta_{v1} = \gamma = \frac{2 - \sigma_v}{\sigma_v} \lambda \quad (2.20)$$

$$\beta_{v2} = \frac{\sigma_v}{2 - \sigma_v} \frac{\gamma^2}{2} \quad (2.21)$$

$$\beta_{t1} = \eta = \frac{2 - \sigma_T}{\sigma_T} \left[\frac{2\beta}{\beta + 1} \right] \frac{1}{\text{Pr}} \lambda \quad (2.22)$$

$$\beta_{t1} = \frac{\text{Pr} \eta^2}{2} \frac{\sigma_T}{2 - \sigma_T} \left[\frac{\beta + 1}{2\beta} \right] \quad (2.23)$$

Where, γ is slip factor and η is jump factor.

2.4 Entropy Generation

The volumetric rate of entropy generation for the steady, axially symmetric, newtonian fluid flow can be written as

$$\dot{S}_{gen}^{\text{vol}} = \dot{S}_{gen,h}^{\text{vol}} + \dot{S}_{gen,f}^{\text{vol}} \quad (2.24)$$

Where $\dot{S}_{gen}^{\text{vol}}$ is the volumetric entropy generation rate per unit volume. $\dot{S}_{gen,h}^{\text{vol}}$ and $\dot{S}_{gen,f}^{\text{vol}}$ are the local volumetric entropy generation rate due to heat transfer and fluid friction, respectively. Steady and axially symmetrical Newtonian fluid-flow entropy generation rate can be expressed in cylindrical coordinates as follow [9];

$$\dot{S}_G^{\text{vol}} = \frac{k}{T_w^2} \left(\frac{\partial T}{\partial z} \right)^2 + \frac{\mu}{T_w} \left\{ 2 \left[\left(\frac{\partial u}{\partial r} \right)^2 + \frac{1}{r^2} u^2 + \left(\frac{\partial w}{\partial z} \right)^2 \right] + \left[\left(\frac{\partial v}{\partial z} \right)^2 + \left(\frac{\partial u}{\partial z} \right)^2 + \left[r \frac{\partial}{\partial r} \left(\frac{v}{r} \right)^2 \right] \right] \right\} \quad (2.25)$$

3. DIFFERENTIAL TRANSFORM METHOD

Differential Transform Method (DTM) is semi-numerical analytical technique that formulized Taylor series in a very different form. The transformation of the kth derivative of a function in one variable is as below [28]

$$F(k) = \frac{1}{k!} \left[\frac{\partial^k f(x)}{\partial x^k} \right]_{x=x_0} \quad (3.1)$$

The inverse transformation is defined as,

$$f(x) = \sum_{k=0}^{\infty} F(k)(x-x_0)^k \quad (3.2)$$

3.1 Theorems

Theorems 1-10, which can be derived equations (3.1) and (3.2) are as follows.

Theorem 1 If $f(x)=g(x)\pm h(x)$ then $F(k) = G(k) \pm H(k)$

Theorem 2 If $f(x) = cg(x)$ then $F(k) = cG(k)$

Theorem 3 If $f(x) = \frac{d^n g(x)}{dx^n}$ then $F(k) = \frac{(k+n)!}{k!} G(k+n)$

Theorem 4 If $f(x) = g(x)h(x)$ then $F(k) = \sum_{k_1=0}^k G(k_1)H(k-k_1)$

Theorem 5 If $f(x) = x^n$ then $F(k) = \delta(k-n)$ where $\delta(k-n) = \begin{cases} 1 & k=n \\ 0 & k \neq n \end{cases}$

Theorem 6 If $f(x) = g_1(x)g_2(x)\dots g_{n-1}(x)g_n(x)$ then

$$F(k) = H(k-k_1) \sum_{k_{n-1}=0}^k \sum_{k_{n-2}=0}^{k_{n-1}} \dots \sum_{k_2=0}^{k_3} \sum_{k_1=0}^{k_2} G_1(k_1)G_2(k_2-k_1)\dots G_{n-1}(k_{n-1}-k_{n-2})G_n(k-k_{n-1})$$

Theorem 7 If $f(x) = g_1(x+a)$ then

$$F(k) = \sum_{h_1=k}^N \binom{h_1}{k} a^{h_1-k} G(h_1) \text{ for } N \rightarrow \infty$$

Theorem 8 If $f(x) = \frac{d^n}{dx^n} [g(x+a)]$ then

$$F(k) = \frac{(k+1)!}{k!} \sum_{h_1=k+n}^N \binom{h_1}{k+n} a^{h_1-k-n} G(h_1) \text{ for } N \rightarrow \infty$$

Theorem 9 If $f(x) = p(x)g^{(n)}(x+a)$ then

$$F(k) = \sum_{k_1=0}^k \sum_{h_1=k-k_1+n}^N \frac{(k-k_1+n)!}{(k-k_1)!} \binom{h_1}{k-k_1+n} a^{h_1-k+k_1-n} P(k_1)G(h_1) \text{ for } N \rightarrow \infty$$

Theorem 10 If $f(x) = g_1^{(n_1)}(x+a_1)g_2^{(n_2)}(x+a_2)$ then

$$F(k) = \sum_{k_1=0}^k \sum_{h_1=k_1+n_1}^N \sum_{h_2=k-k_1+n_2}^N \frac{(k_1+n_1)!(k-k_1+n_2)!}{k_1! (k-k_1)!} \binom{h_1}{k_1+n_1} \binom{h_2}{k-k_1+n_2} a_1^{h_1-k_1-n_1} a_2^{h_2-k+k_1-n_2} G_1(h_1)G_2(h_2) \text{ for } N \rightarrow \infty$$

4. ANALYSIS AND SOLUTION OF EQUATIONS

4.1 Transform of The Equations

4.1.1 Flow Field

Von Karman dimensionless axial coordinate $\zeta = z\sqrt{\Omega/\nu}$ is introduced together with the following velocity components and pressure.[1]

$$u = \Omega r F(\zeta), \quad v = \Omega r G(\zeta), \quad w = \sqrt{\Omega \nu} H(\zeta), \quad p = -\rho \Omega \nu P(\zeta) \quad (4.1)$$

Equations (2.6), (2.7), (2.8) and (2.9) can be non-dimensionalized with equation (4.1) as follows,

$$F'' = HF' + F^2 - G^2 \quad (4.2)$$

$$G'' = HG' + 2FG \quad (4.3)$$

$$H' = -2F \quad (4.4)$$

$$P'' = HH' - H'' \quad (4.5)$$

The slip boundary conditions for the considered problem are introduced as follows;

$$u = \beta_{v1} \frac{\partial u}{\partial z} + \beta_{v2} \frac{\partial^2 u}{\partial z^2}, \quad v = r\Omega + \beta_{v1} \frac{\partial v}{\partial z} + \beta_{v2} \frac{\partial^2 v}{\partial z^2}, \quad w = W \quad \text{at } z=0 \quad (4.6)$$

$$u \rightarrow 0, \quad v \rightarrow 0 \quad \text{as } z \rightarrow \infty \quad (4.7)$$

Where $W = w_0 / \sqrt{\omega \nu}$ is the uniform suction or blowing parameter. For suction case, this parameter takes constant negative values and for blowing case, this parameter takes positive constant values.

Boundary conditions in equations (4.6)-(4.7) can be written as follow by using Von Karman dimensionless coordinate system,

$$F(0) = \beta_{v1}F'(0) + \beta_{v2}F''(0), \quad G(0) = 1 + \beta_{v1}G'(0) + \beta_{v2}G''(0), \quad H(0) = W \quad (4.8)$$

$$F(\infty) = 0, \quad G(\infty) = 0 \quad (4.9)$$

In an effort to transform infinite ζ range to finite ξ range, the following dependent and independent variables are used. This method firstly introduced by Benton [29].

$$\xi = e^{-c\zeta} \quad (4.10)$$

$$F(\zeta) = c^2 f(\xi), \quad G(\zeta) = c^2 g(\xi), \quad H(\zeta) = W - c[1 - h(\xi)] \quad (4.11)$$

Equations (4.2)-(4.5) can be rewritten as below by using transformation in quations (4.10)-(4.11).

$$\xi^2 f''(\xi) = f^2(\xi) - g^2(\xi) - \xi f'(\xi)h(\xi) \quad (4.12)$$

$$\xi^2 g''(\xi) = 2f(\xi)g(\xi) - \xi g'(\xi)h(\xi) \quad (4.13)$$

$$\xi h'(\xi) = 2f(\xi) \quad (4.14)$$

Comparably, boundary conditions (4.8)-(4.9) become as follow,

$$f(1) = -\beta_{v1}cf'(1) + \beta_{v2}c^2 f''(1), \quad g(1) = c^{-2} - \beta_{v1}cg'(1) + \beta_{v2}c^2 g''(1), \quad h(1) = 1 \quad (4.15)$$

$$f(0) = 0, \quad g(0) = 0 \quad (4.16)$$

4.1.2 Thermal Field

Dimensionless temperature for rotating disk flow is defined as follows,

$$\theta = \frac{T - T_\infty}{T_w - T_\infty} \quad (4.17)$$

Where T_∞ is temperature at infinity, T_w is temperature on the disk. Equation (2.11) becomes as follows by using dimensionless form in equation (4.17).

$$\theta'' = PrH\theta' \quad (4.18)$$

Where Pr is the Prandtl Number. Comparably, by using equation (4.17) boundary condition in equation (2.19) becomes as follows:

$$\theta(\infty) = 0, \quad \theta(0) = 1 + \beta_{t1}\theta'(0) + \beta_{t2}\theta''(0) \quad (4.19)$$

ϕ is the generalized thermal jump factor can be defined as follows;

$$\phi = \beta_{t1} + \beta_{t2} Pr W \quad (4.20)$$

Integrating equation (4.18) and implementing the second boundary condition in equation (4.19) then dimensionless temperature can be defined in terms of the axial component of the velocity field as follows;

$$\theta(\zeta) = \theta'(0) \left(\int_0^\zeta e^{-\int_0^\chi Pr H(\alpha) d\alpha} d\chi + \phi \right) + 1 \quad (4.21)$$

In addition, the missing boundary condition $\theta'(0)$ is evaluated by equation (4.21) together with the first boundary condition in equation (4.19) as follows;

$$\theta'(0) = -1 / \left(\int_0^\infty e^{-\int_0^\chi Pr H(\alpha) d\alpha} d\chi + \phi \right) \quad (4.22)$$

After solving the flow field, the thermal field is determined from equations (4.21)-(4.22) by using numerical integration.

4.1.3 Entropy Generation

Using dimensionless variables in equation (4.1), equation (2.24) can be written as in simple terms as follow [9];

$$N_g = Re \theta'(\zeta)^2 + \psi \left\{ 3 Re^2 H'(\zeta)^2 + Re^3 \bar{r}^2 \left[G'(\zeta)^2 + F'(\zeta)^2 \right] \right\} \quad (4.23)$$

Where $Re = \Omega R^2 / \nu$ is the rotational Reynolds number, $Br = \mu \Omega^2 R^2 / k \Delta T$ is the rotational Brinkman number, $\beta = \Delta T / \bar{T}$ is the dimensionless temperature difference,

$\bar{r} = r/R$ is the dimensionless radial coordinate and $\psi = Br/\alpha Re^2$ is called the group parameter. It helps us to compare the relative importance of viscous effects and heat transfer irreversibility.

The total local entropy generation in equation (4.23) can be written as the summation of local entropy generation due to heat transfer irreversibility (N_H), which is the first term and the local entropy generation due to fluid friction irreversibility (N_F), which is the second term on the right-hand side.

$$N_G = N_H + N_F \quad (4.24)$$

It may be possible to evaluate these terms individually then check against them to see the dominance of one term on the other. Local entropy generation because of heat transfer (N_H) includes the entropy generation by heat transfer due to axial conduction from the rotating disk. Local entropy generation because of fluid friction contains velocity gradients in axial, radial and circumferential directions.

The irreversibility distribution ratio (Φ) is the first dimensionless parameter in the entropy generation analysis of convective heat transfer problem. This ratio shows the ratio between the entropy generation due to fluid friction and heat transfer. The irreversibility distribution ratio can be written as follows: [9,13]

$$\Phi = \frac{N_F}{N_H} = \frac{\psi \left\{ 3Re H'(\zeta)^2 + Re^2 \bar{r}^2 \left[G'(\zeta)^2 + F'(\zeta)^2 \right] \right\}}{T'(\zeta)^2} \quad (4.25)$$

In the range $0 < \Phi < 1$, heat transfer irreversibility is dominant and when $\Phi > 1$, fluid friction dominates the entropy generation. When $\Phi = 1$, the contributions of heat transfer and fluid friction to entropy generation are equal. Another alternative irreversibility distribution parameter is the Bejan number (Be), which is the ratio of entropy generation due to heat transfer to the total entropy generation. This number is given in dimensionless form as follows [31]:

$$Be = \frac{N_H}{N_G} = \frac{1}{1 + \Phi} = \frac{T'(\zeta)^2}{T'(\zeta)^2 + \psi \left\{ 3Re H'(\zeta)^2 + Re^2 \bar{r}^2 \left[G'(\zeta)^2 + F'(\zeta)^2 \right] \right\}} \quad (4.26)$$

In the range $0 < Be < 1$ and the specific value of $Be = 1$ corresponds to a condition, where the heat transfer irreversibility totally dominates and for $Be = 0$ fluid friction effects totally dominate the entropy generation. For $Be \leq 1/2$, the irreversibility caused by viscous effects dominates and for $Be \geq 1/2$, the irreversibility caused by heat transfer is dominant. When $Be = 1/2$, the heat transfer and the fluid friction entropy generation rates are equal.

The dimensionless volumetric entropy generation rate, which is an important measure of the total global entropy generation, can be written as:

$$N_{G,av} = \frac{1}{\nabla} \int_0^m \int_0^1 2\pi\bar{r}N_G d\bar{r}d\zeta \quad (4.27)$$

Where ∇ is the volume considered. Since the gradients in velocity and thermal fields exponentially decrease with increasing ζ , consideration of the complete flow domain results in zero volumetric entropy generation. The integration in equation (4.27) is obtained in the domain $0 \leq \bar{r} \leq 1$ and $0 \leq \zeta \leq m$, where m is a adequately large number. It can be introduced that the average Bejan number as follows.

$$Be_{av} = \frac{1}{\nabla} \int_0^m \int_0^1 2\pi\bar{r}Be d\bar{r}d\zeta \quad (4.28)$$

4.2 Solution of The Equations

We applied differential transform method (DTM) to the equations (4.12) – (4.14) and used B.C.'s in equations (4.15)-(4.16) at $\xi = 0$. By using DTM theorems, the differential transform of equations (4.15)-(4.16) can be calculated as follows:

$$\tilde{F}(k) = \frac{1}{k(k-1)} \sum_{l=0}^k \left[\tilde{F}(l)\tilde{F}(k-l) - \tilde{G}(l)\tilde{G}(k-l) - l\tilde{F}(l)\tilde{H}(k-l) \right] \quad (4.29)$$

$$\tilde{G}(k) = \frac{1}{k(k-1)} \sum_{l=0}^k \left[2\tilde{F}(l)\tilde{G}(k-l) - l\tilde{G}(l)\tilde{H}(k-l) \right] \quad (4.30)$$

$$\tilde{H}(k) = \frac{2}{k} \tilde{F}(k) \quad (4.31)$$

Where, $k \geq 2$ and $\tilde{F}(k)$, $\tilde{G}(k)$ and $\tilde{H}(k)$ denote to the differential transform of $f(\xi)$, $g(\xi)$ and $h(\xi)$ respectively. For determining the dependent variables, we need to know the unknown B.C.'s $f'(0)$ and $g'(0)$. First, the values of $\tilde{F}(k)$, $\tilde{G}(k)$, $\tilde{H}(k)$ for $k = 2, 3, \dots, N$ in terms of $f'(0)$, $g'(0)$, which will be called as f_1, g_1 respectively, are obtained and then by using the boundary conditions given in equation (4.15) for $\xi = 1$, we calculated f_1 , g_1 and c numerically. This is much faster and cost efficient than the numerical techniques since it is not iterative. The boundary conditions given in equation (4.16) for $\xi = 0$ are transformed as follows:

$$\tilde{F}(0) = 0, \tilde{G}(0) = 0, \tilde{H}(0) = 0 \text{ and } \tilde{F}(1) = f_1, \tilde{G}(1) = g_1 \quad (4.32)$$

By using the inverse relations in equations (4.29)-(4.31) and the transformed boundary conditions in equation (4.32), $\tilde{F}(k)$, $\tilde{G}(k)$ and $\tilde{H}(k)$ for $k = 2, 3, \dots, N$ are evaluated. Then, using the inverse transformation rule in [12], the series solutions are obtained from:

$$f(\xi) = \sum_{k=0}^N \tilde{F}(k) \xi^k, \quad g(\xi) = \sum_{k=0}^N \tilde{G}(k) \xi^k, \quad h(\xi) = \sum_{k=0}^N \tilde{H}(k) \xi^k \quad (4.33)$$

where, N is the number of terms to be evaluated. By calculating up to $N = 7$, we get:

$$\begin{aligned} f(\xi) = & f_1 \xi + \left(-\frac{f_1^2}{2} - \frac{g_1^2}{2}\right) \xi^2 + \left(\frac{f_1^3}{4} + \frac{f_1 g_1^2}{4}\right) \xi^3 + \\ & \left(-\frac{17f_1^4}{144} - \frac{f_1^2 g_1^2}{8} - \frac{g_1^4}{144}\right) \xi^4 + \left(\frac{61f_1^5}{1152} + \frac{37f_1^3 g_1^2}{576} + \frac{13f_1 g_1^4}{1152}\right) \xi^5 + \\ & \left(-\frac{73f_1^6}{3200} - \frac{113f_1^4 g_1^2}{3456} - \frac{889f_1^2 g_1^4}{86400} - \frac{7g_1^6}{17280}\right) \xi^6 \end{aligned} \quad (4.34)$$

$$\begin{aligned} g(\xi) = & g_1 \xi + \left(-\frac{f_1^2 g_1}{12} - \frac{g_1^3}{12}\right) \xi^3 + \left(\frac{f_1^3 g_1}{18} + \frac{f_1 g_1^3}{18}\right) \xi^4 + \\ & \left(-\frac{53f_1^4 g_1}{1920} - \frac{29f_1^2 g_1^3}{960} - \frac{g_1^5}{384}\right) \xi^5 + \left(\frac{13f_1^5 g_1}{1080} + \frac{41f_1^3 g_1^3}{2700} + \frac{17f_1 g_1^5}{5400}\right) \xi^6 \end{aligned} \quad (4.35)$$

$$\begin{aligned}
h(\xi) = & 2f1\xi + \left(-\frac{f1^2}{2} - \frac{g1^2}{2}\right)\xi^2 + \left(\frac{f1^3}{6} + \frac{f1g1^2}{6}\right)\xi^3 + \\
& \left(-\frac{17f1^4}{288} - \frac{f1^2g1^2}{16} - \frac{g1^4}{288}\right)\xi^4 + \left(\frac{61f1^5}{2880} + \frac{37f1^3g1^2}{1440} + \frac{13f1g1^4}{2880}\right)\xi^5 + \\
& \left(-\frac{73f1^6}{9600} - \frac{113f1^4g1^2}{10368} - \frac{889f1^2g1^4}{259200} - \frac{7g1^6}{51840}\right)\xi^6
\end{aligned} \tag{4.36}$$

After calculating $f(\xi)$, $g(\xi)$ and $h(\xi)$ the original dependent variables $F(\zeta)$, $G(\zeta)$ and $H(\zeta)$ are obtained by using equations (4.10)-(4.11).

5. EFFECT OF SECOND ORDER VELOCITY SLIP AND TEMPERATURE JUMP CONDITIONS ON ROTATING DISK FLOW IN CASE OF BLOWING AND SUCTION WITH ENTROPY GENERATION

Effect of second order velocity slip and temperature jump boundary conditions is examined in three subtitles. Blowing, suction and neutral cases are considered in flow field, temperature field and entropy generation.

5.1 Flow Field

After solution of the flow field, radial, circumferential and axial velocity profiles plotted in Fig 5.1-5.3.

The upper side of Fig 5.1 illustrates the variation of radial velocity with respect to ζ for first order and second order slip effects in case of difference slip factors. Differently from no-slip regime, the flow has radial velocity on disk surface in slip flow regime.

The lower side of the Fig 5.1 illustrates the variations of the dimensionless radial velocity profile by carrying out the first and second order boundary conditions. Radial flow velocity ($F(\zeta)$) on the disk surface and the velocity of the disk itself become different in the slip-flow regime. While the slip factor takes greater values, the velocity gradient reduces.

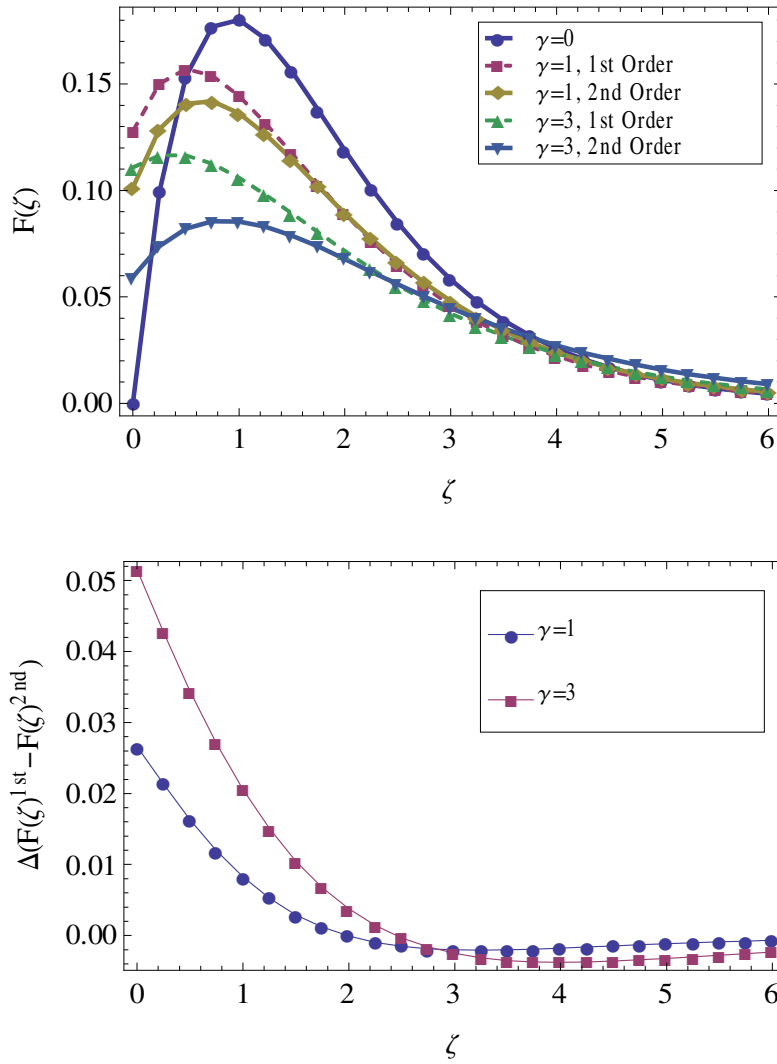


Figure 5.1 : Variation of $F(\zeta)$ with respect to ζ for first order and second order slip.

Difference between first and second order value of $F(\zeta)$ with respect to ζ .

The upper side of Fig 5.2 illustrates the dimensionless circumferential velocity in case of different slip factors. The lower side of the Fig 5.2 illustrates the variations of the dimensionless circumferential velocity profile by carrying out the first and second order boundary conditions. Similarly, circumferential flow velocity ($G(\zeta)$) and the disk velocity show a deviation when the slip factor increases. The maximum difference between first and second order boundary conditions occurs about $\zeta=2$ as shown in lower side of Fig. 5.2

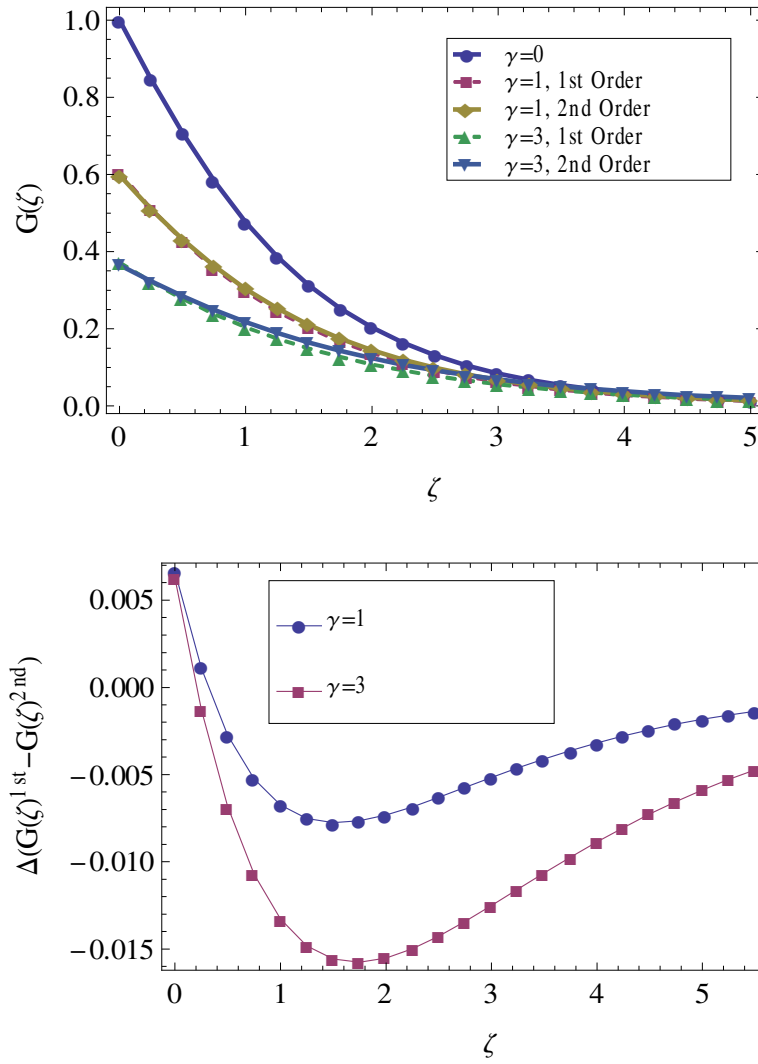


Figure 5.2 : Variation of $G(\zeta)$ with respect to ζ for first order and second order slip.
 Difference between first and second order value of $G(\zeta)$ with respect to ζ .

The upper side of Fig 5.3 illustrates the dimensionless axial velocity in case of different slip factors. The lower side of the Fig 5.3 illustrates the variations of the dimensionless axial velocity profile by carrying out the first and second order boundary conditions. The maximum difference between first and second order boundary conditions occurs about $\zeta=2-3$ as shown in lower side of Fig. 5.3

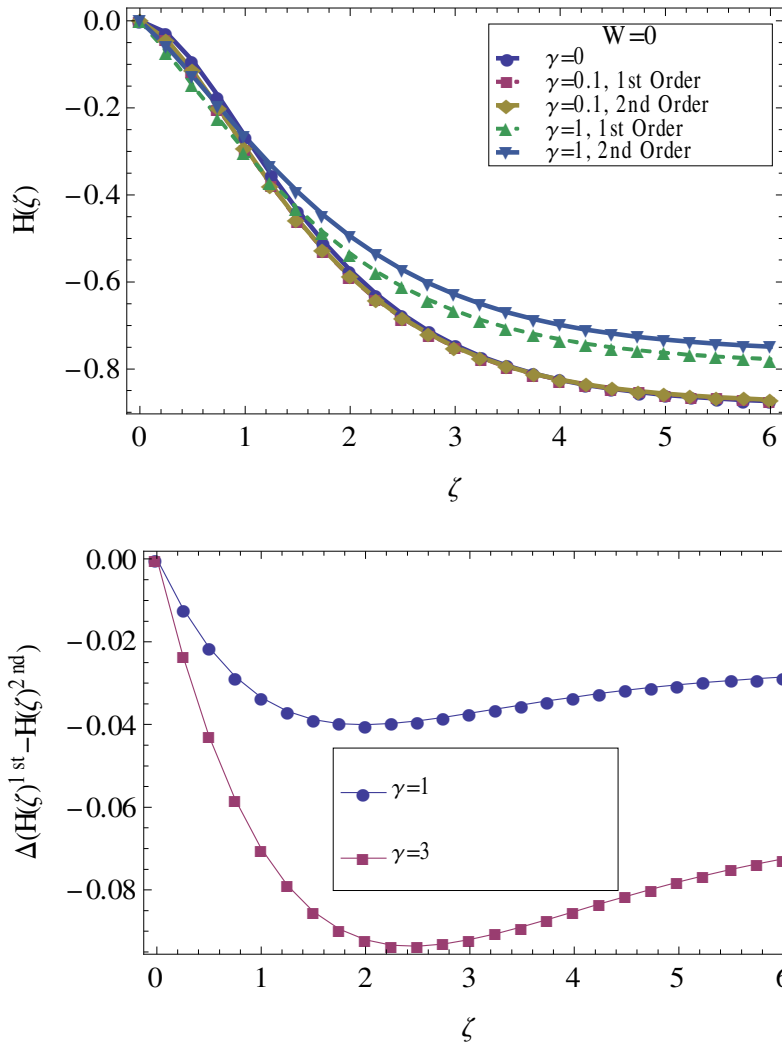


Figure 5.3 : Variation of $H(\zeta)$ with respect to ζ for first order and second order slip.

Difference between first and second order value of $H(\zeta)$ with respect to ζ .

5.2 Thermal Field

The variation of temperature with respect to ζ for first order and second order slip and differences occur by applying first and second order boundary conditions as presented in Fig. 5.4.

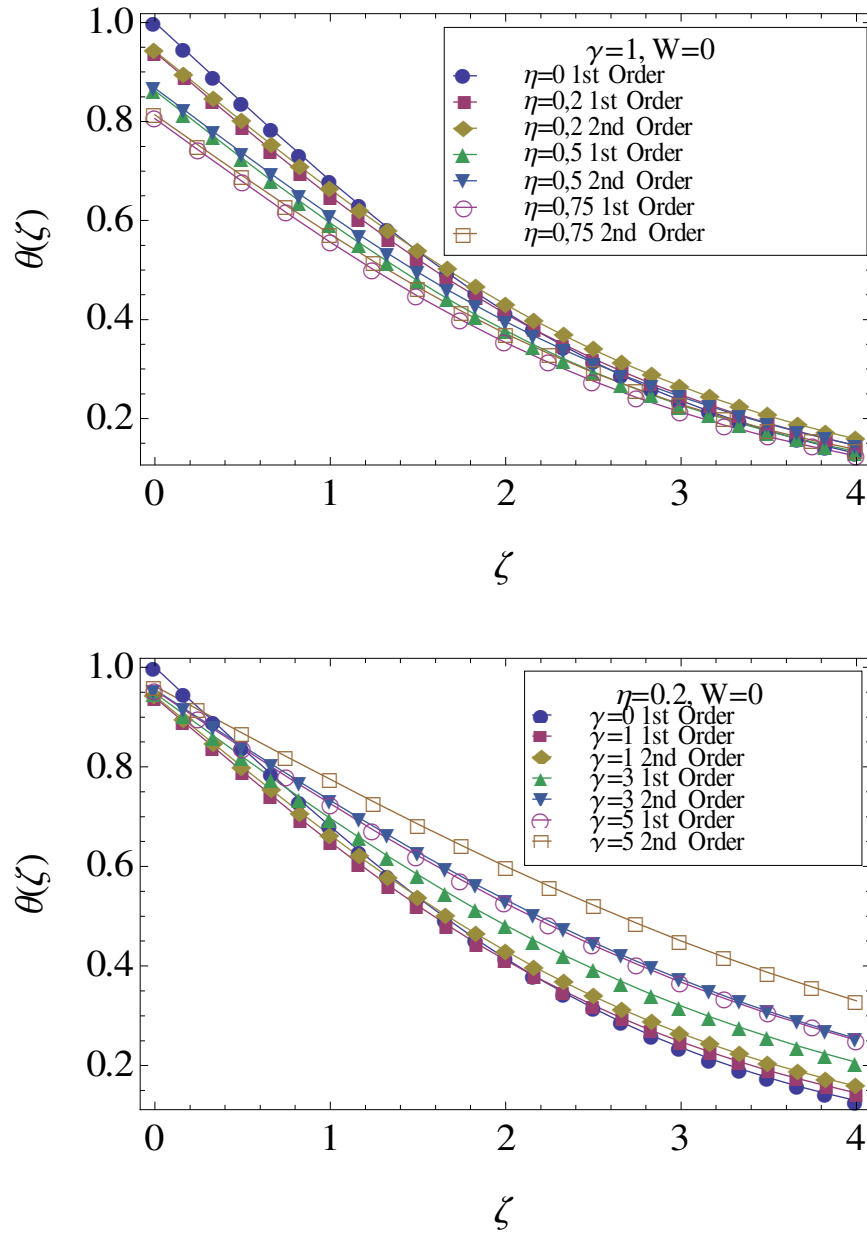


Figure 5.4 : Variation of $\theta(\zeta)$ with respect to ζ for first order and second order slip.
 Difference between first and second order value of $\theta(\zeta)$ with respect to ζ .

The upper side of Fig. 5.4 shows the variation of temperature field in several jump factors. The lower side of Fig. 5.4 shows the variation of temperature field in several slip factors. Increasing jump factor raise the temperature deviation between disk and adjacent flow. Additionally increasing jump and slip factors reduce the temperature gradient.

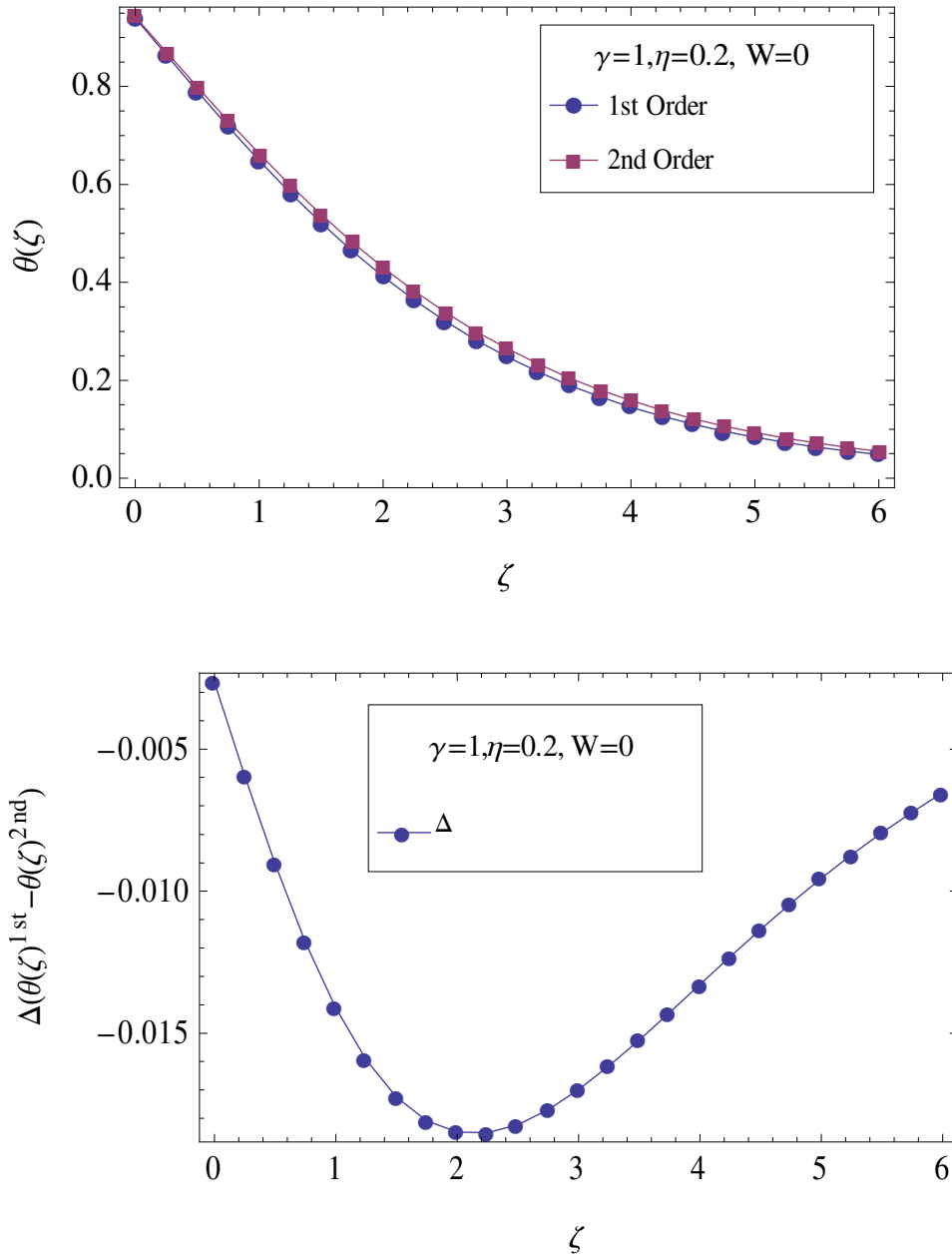


Figure 5.5 : Variation of $\theta(\zeta)$ with respect to ζ for first order and second order slip in Neutral case ($W=0$). Difference between first and second order value of $\theta(\zeta)$ with respect to ζ .

After solving the dimensionless temperature profile, results for neutral, suction and blowing case are plotted in Fig.5.5-5.7. The most difference between the effects of applying first and second order boundary condition occurs in blowing case.

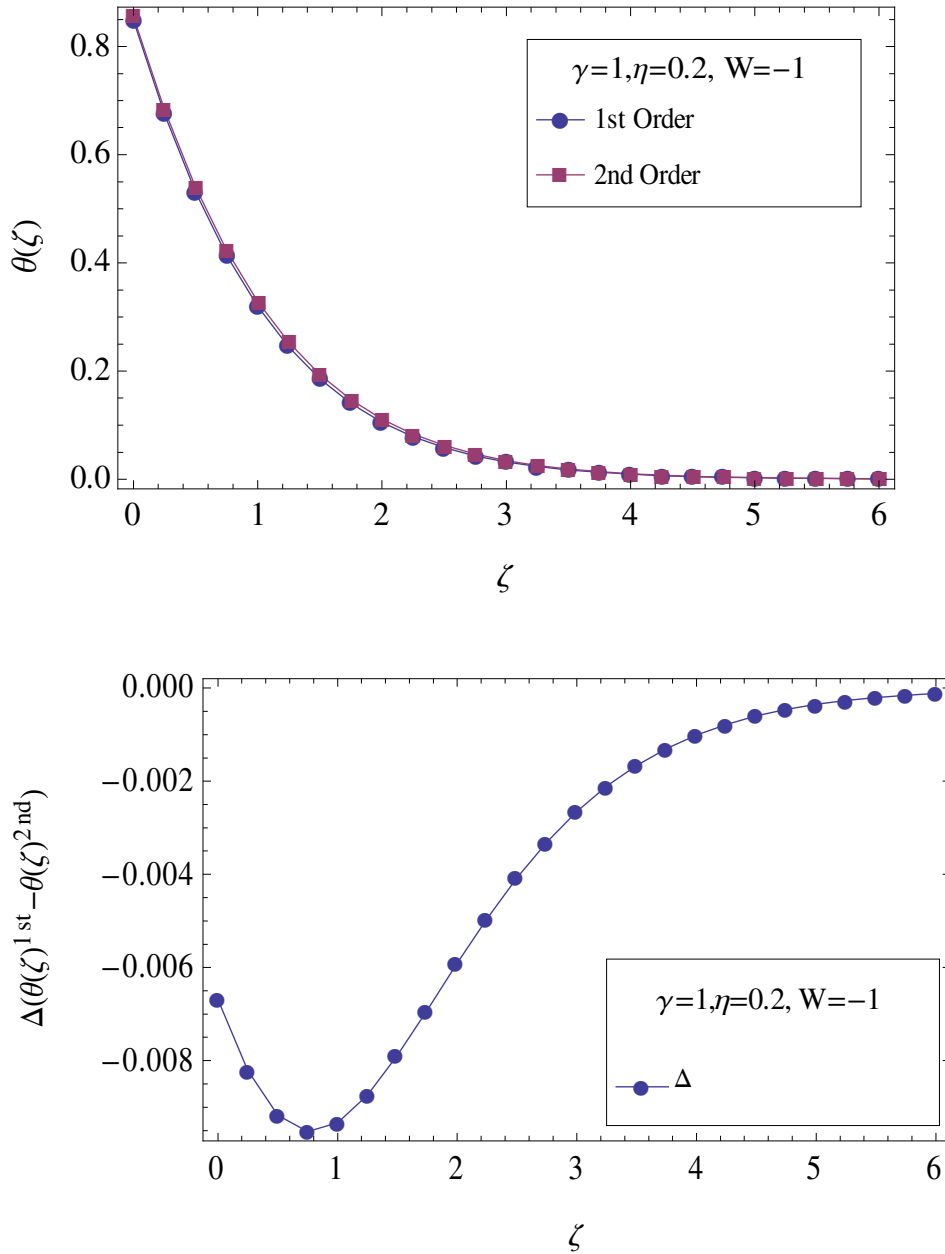


Figure 5.6 : Variation of $\theta(\zeta)$ with respect to ζ for first order and second order slip in Suction case ($W=-1$). Difference between first and second order value of $\theta(\zeta)$ with respect to ζ .

In the suction case ($W=-1$) shown in Fig.5.6, the temperature sharply decreases away from the disk surface, however for the blowing case ($W=1$) shown in Fig. 5.7 the temperature is almost constant along the ζ -axis then it takes the decreasing trend after $\zeta = 15$. For suction and neutral cases shown in Fig. 5.5 and Fig. 5.7, the first and second order effects are closer and second order effects are negligible.

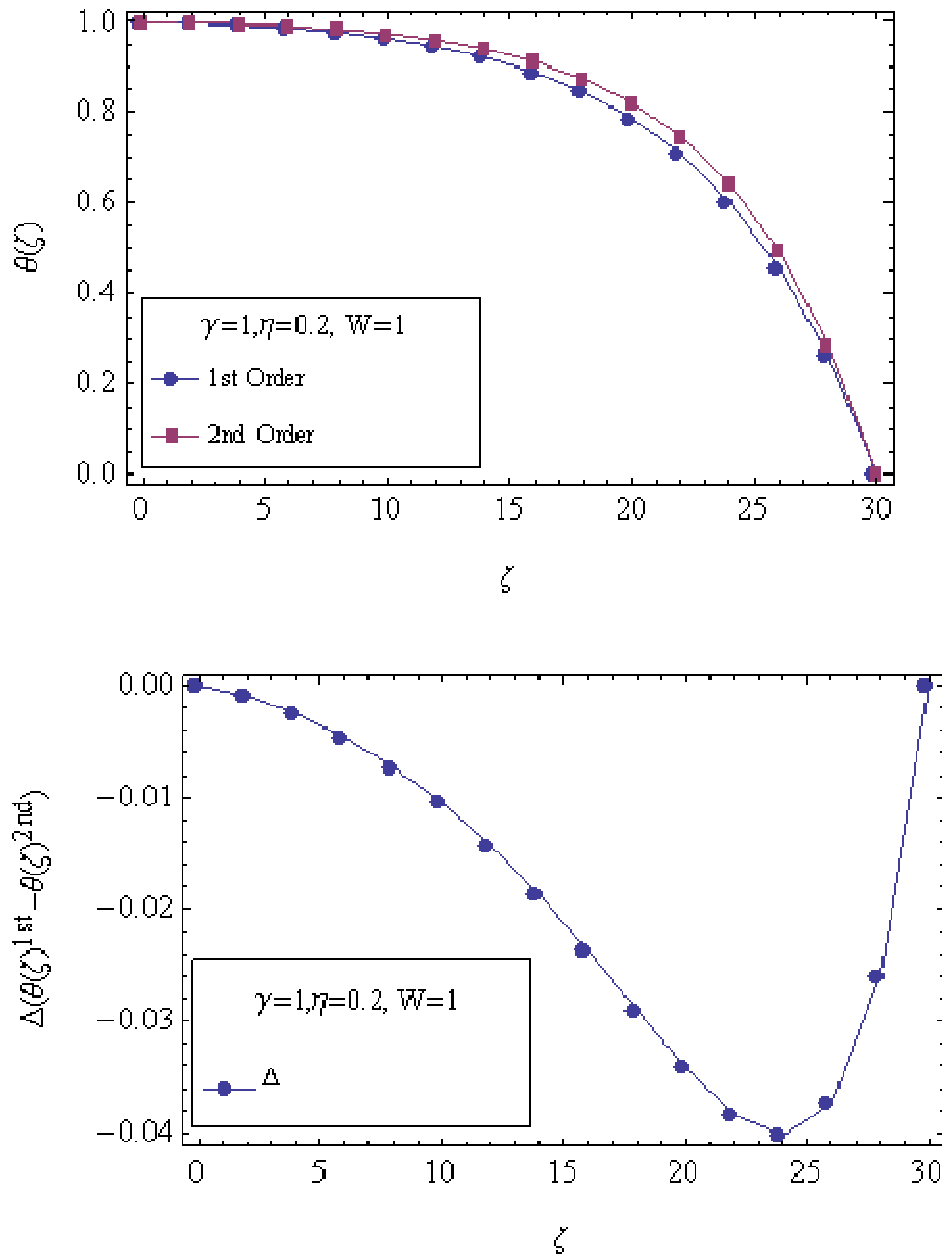


Figure 5.7 : Variation of $\theta(\zeta)$ with respect to ζ for first order and second order slip in Blowing case ($W=1$). Difference between first and second order value of $\theta(\zeta)$ with respect to ζ .

If the temperature distributions in the flow fields are represented greater than two degree polynomial, second order boundary condition approach would have to be used [11].

5.3 Entropy Generation

Local entropy generation rates are shown in Fig. 5.8-5.10.

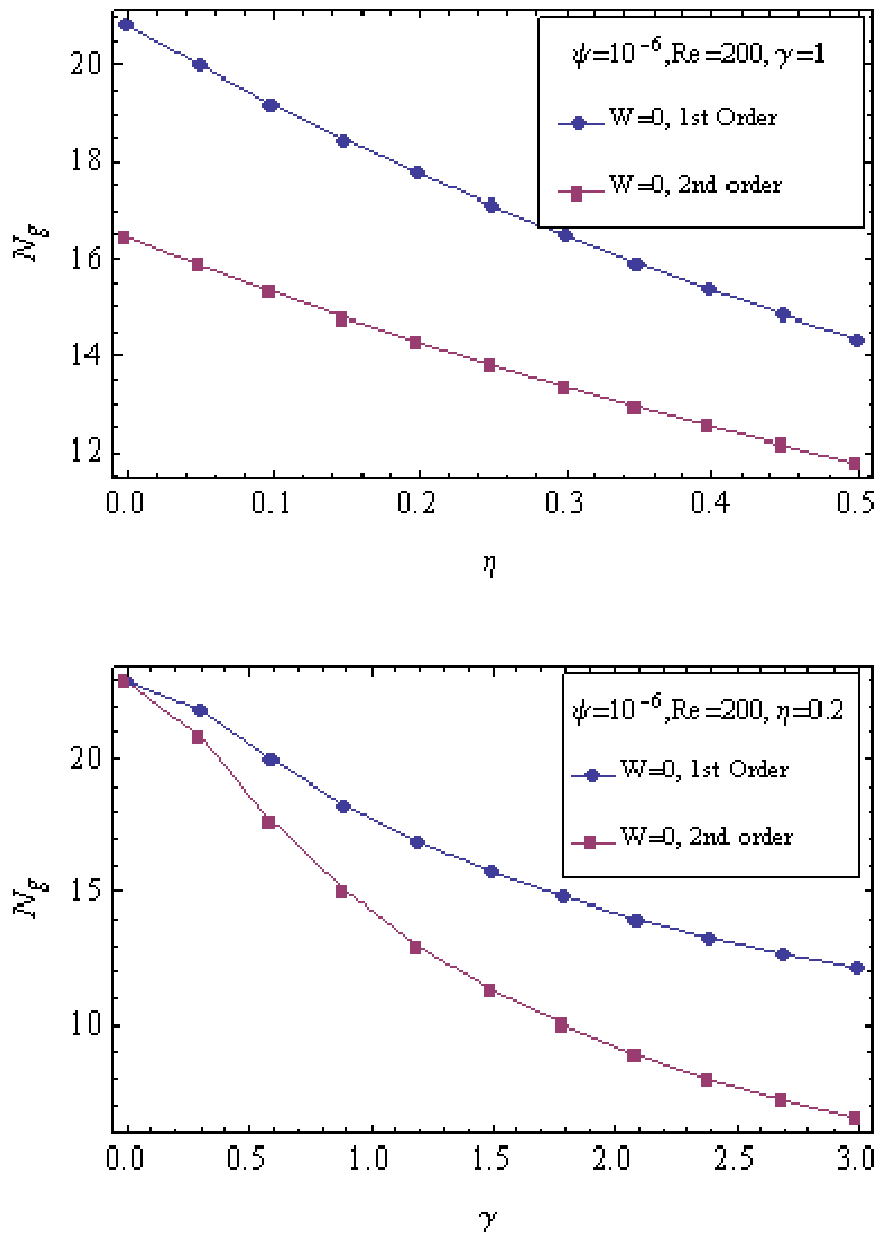


Figure 5.8 : Variation of N_g with respect to slip factor and jump factor ($\bar{\tau}=1$) in Neutral case ($W=0$)

While slip and jump factors take greater values, the local entropy generation rates reduce. Excluding blowing case ($W=1$), the local entropy generation rate show a noticeable difference for the first and the second order boundary conditions (Fig. 5.8-5.9).

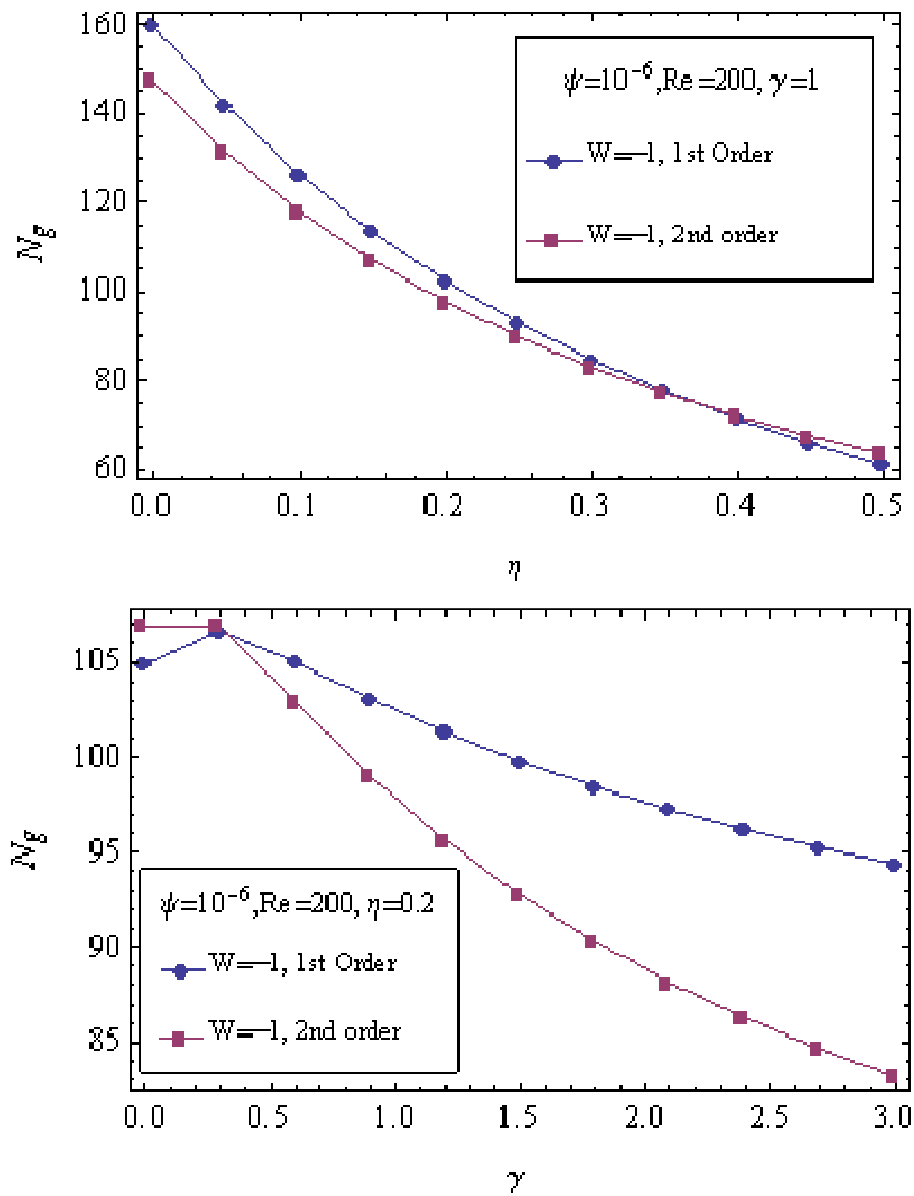


Figure 5.9 : Variation of N_g with respect to slip factor and jump factor ($\bar{\tau}=1$) in Suction case ($W=-1$)

Local entropy generation rates are shown in Fig. 5.8-5.10. While slip and jump factors take greater values, the local entropy generation rates reduce. Excluding blowing case ($W=1$), the local entropy generation rate show a noticeable difference for the first and the second order boundary conditions (Fig. 5.8-5.9).

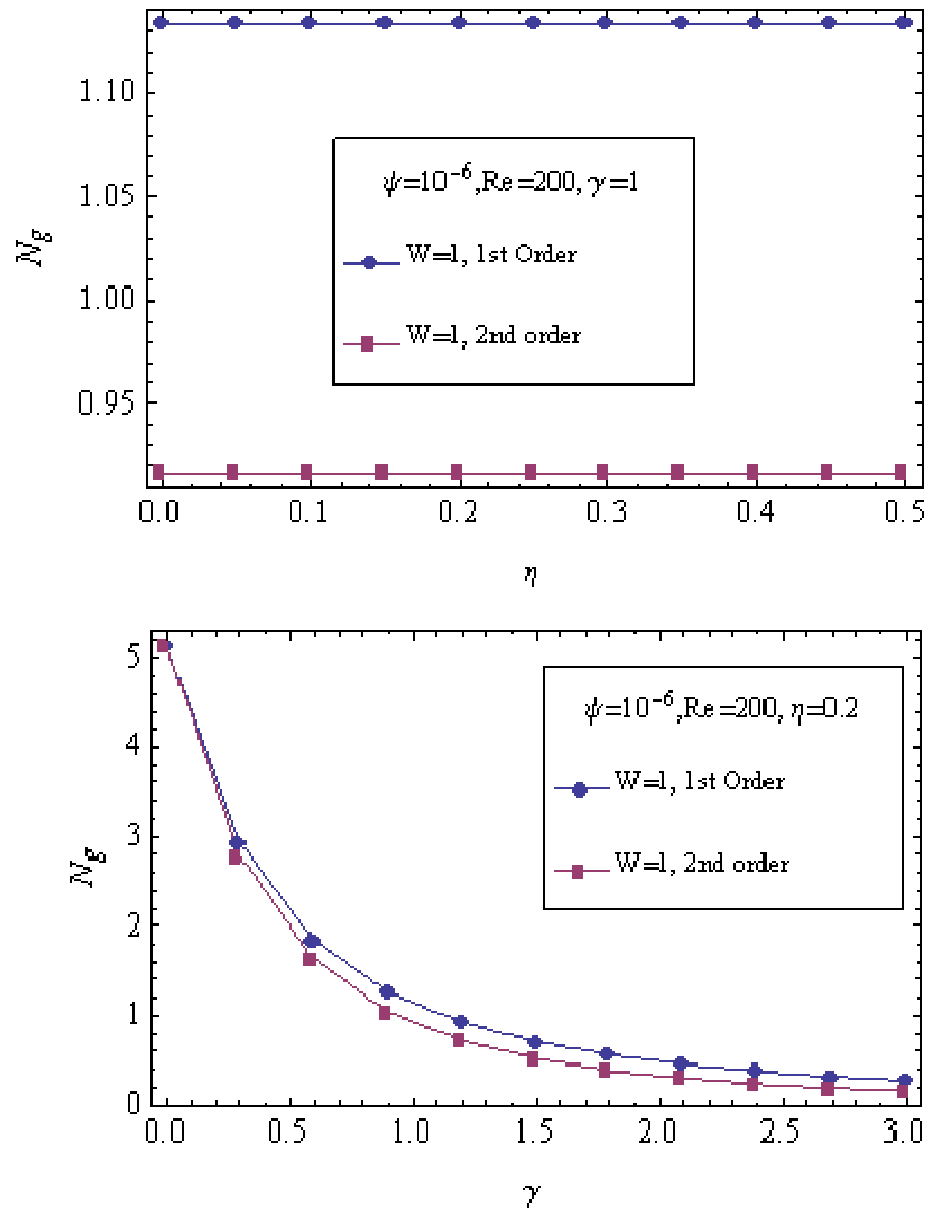


Figure 5.10 : Variation of N_g with respect to slip factor and jump factor ($\bar{\tau}=1$) in Blowing case ($W=1$)

In neutral, suction and blowing cases, the change of $N_{g,av}$ with respect to slip and jump factors for first and second order are shown in Fig. 5.11-5.13. The rarefied effect reduces the velocity gradients in all directions and consequently as the temperature gradient in the entire flow field. This situation causes a reduction in the volumetric entropy generation rate.

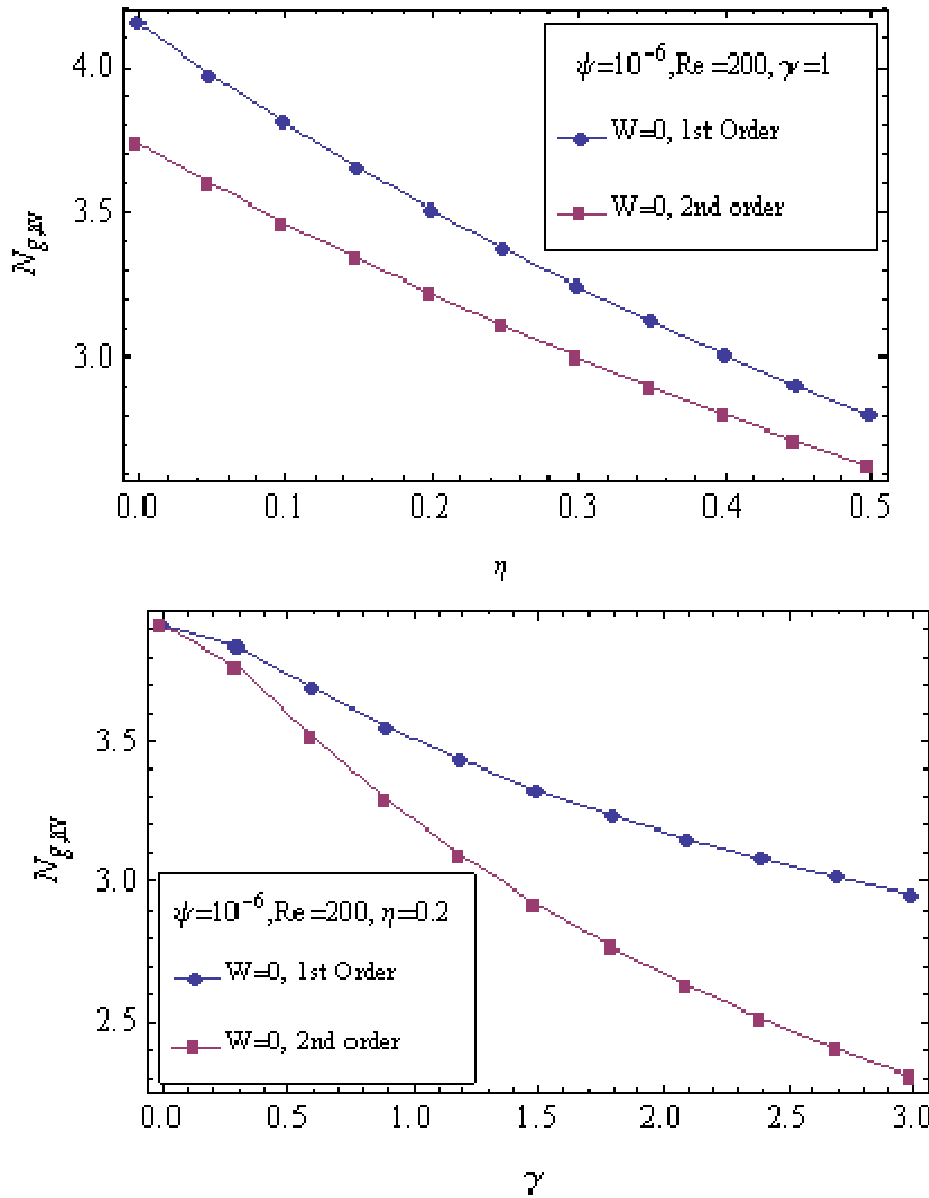


Figure 5.11 : Variation of $N_{g,av}$ with respect to slip factor and jump factor for first and second order in Neutral case ($W=0$)

For the cases $W=1$ as well as $W=0$ and $W=-1$, the entropy generation must be carried out in volumetric measure to get a sense about the total entropy generation. It has been observed from Fig. 5.11-5.13 that using the second order boundary conditions results in lower entropy generation comparing to first order boundary condition case. It means that it is possible to reduce entropy generation and increase system efficiency. This result is paramount importance for the design of fluidic systems.

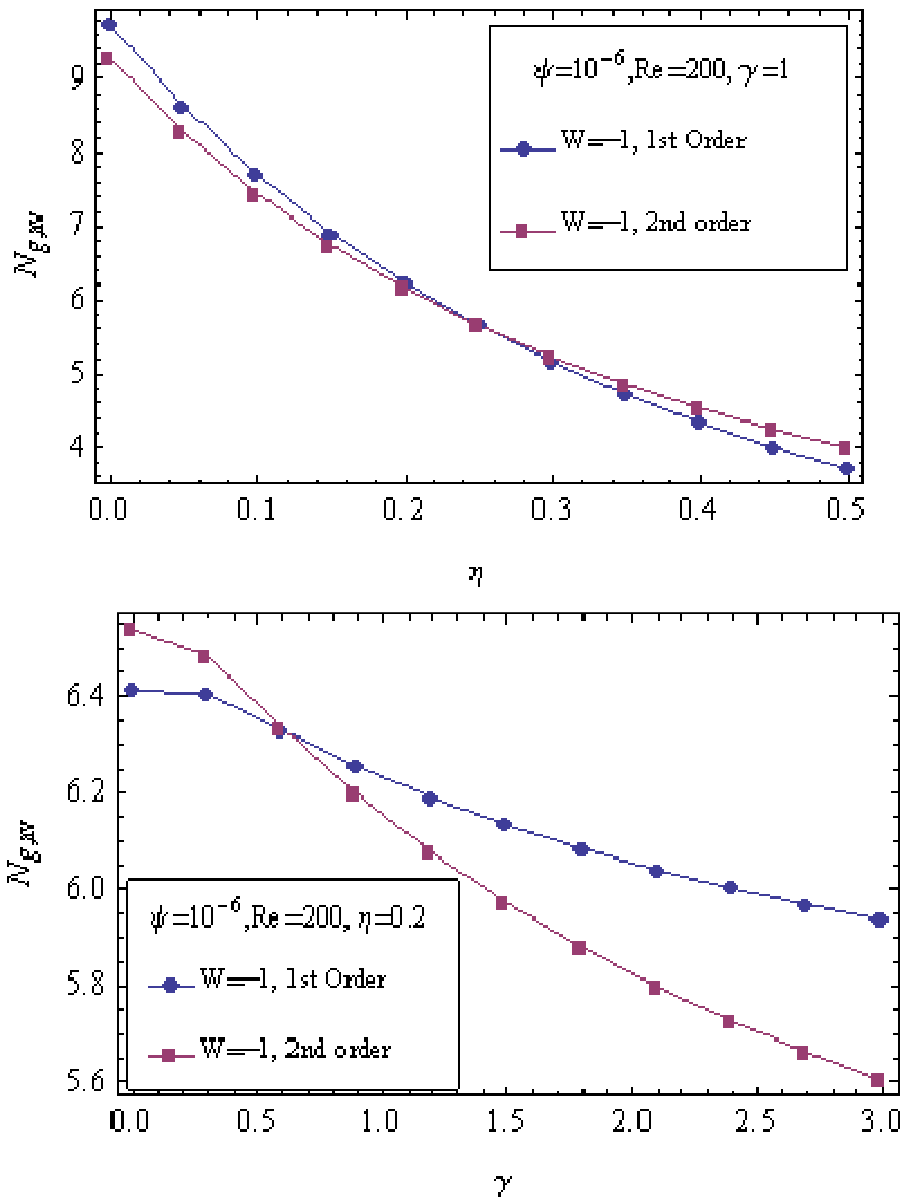


Figure 5.12 : Variation of $N_{g,av}$ with respect to slip factor and jump factor for first and second order in Suction case ($W=-1$)

In neutral, suction and blowing conditions, the local entropy generation rate is illustrated as 3-D in Fig.5.14-5.16. Maximum local entropy generation rate occurs on disk surface and local entropy generation rate reduces away the disk surface.

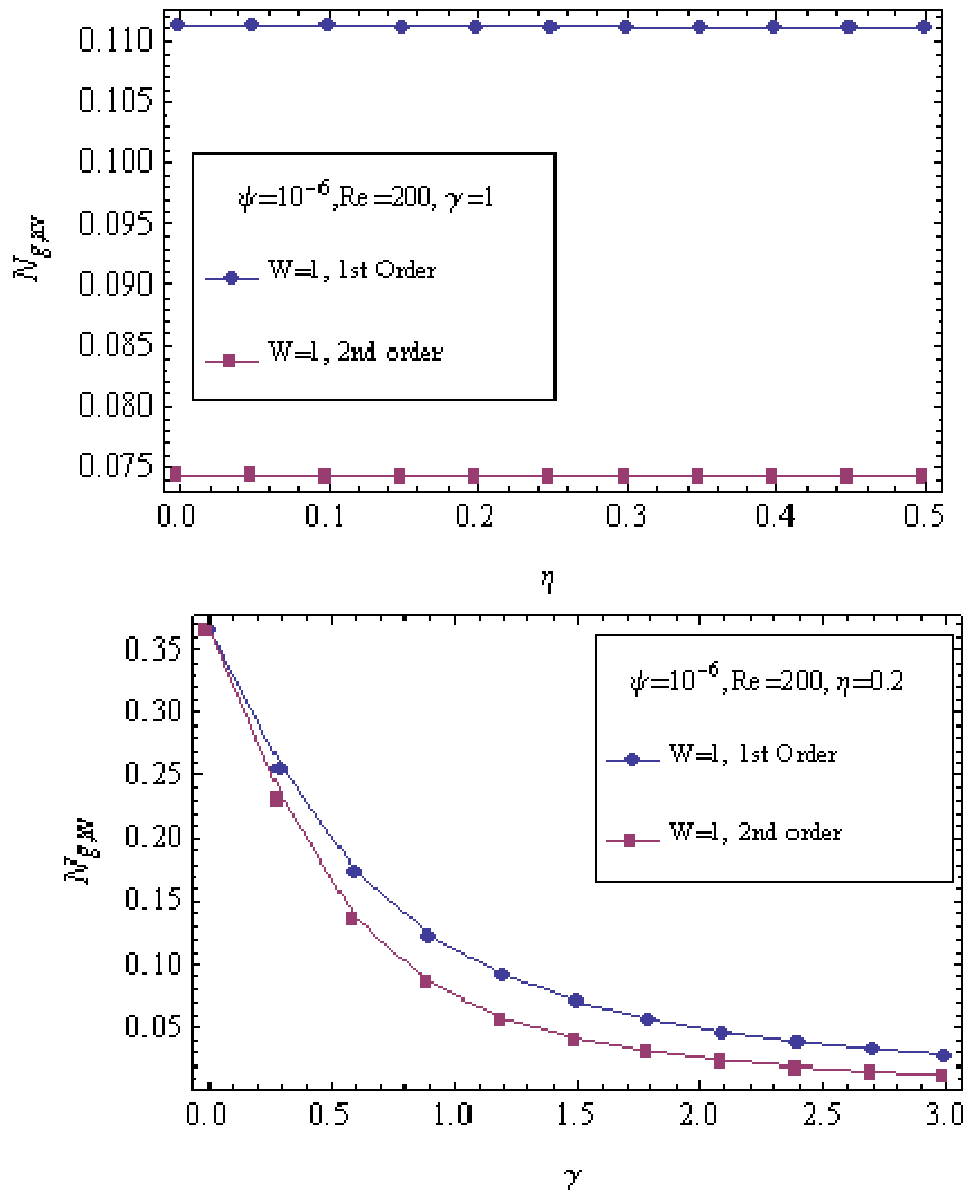
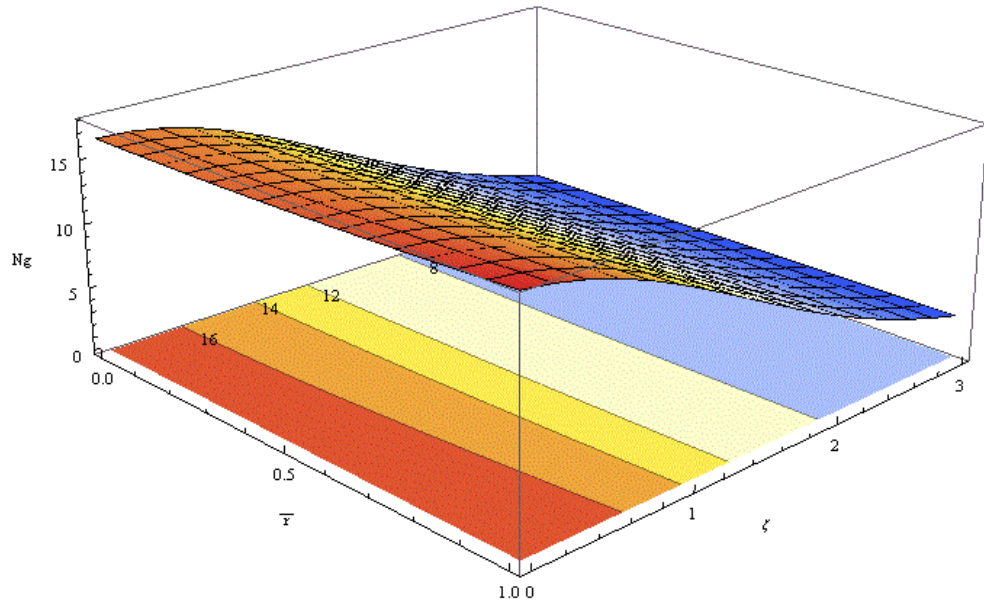
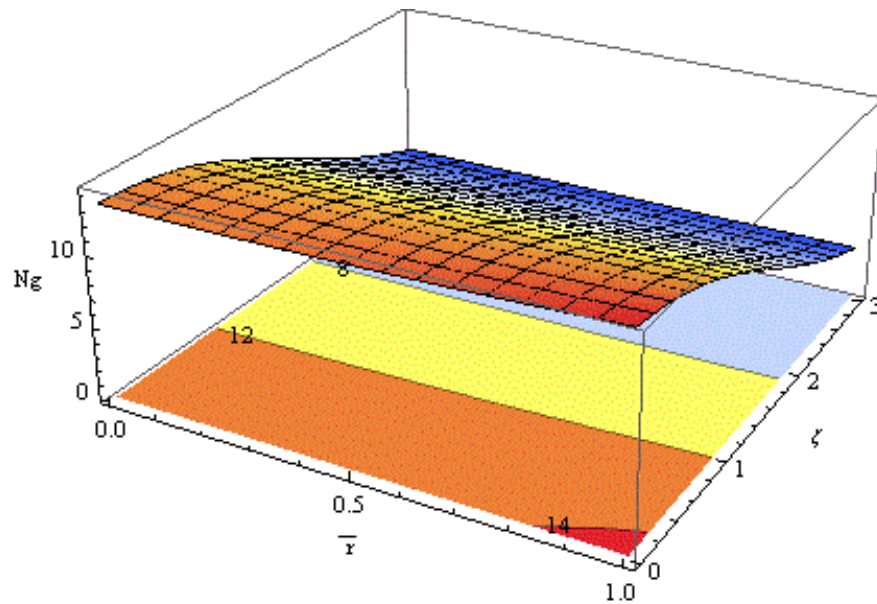


Figure 5.13 : Variation of $N_{g,av}$ with respect to slip factor and jump factor for first and second order in Blowing case ($W=1$)

Local entropy generation rate is decreases when the second order velocity slip and temperature jump conditions are used. Local entropy generation on disk surface increases to the radial direction and takes its maximum value when the dimensionless disk radius reach 1.



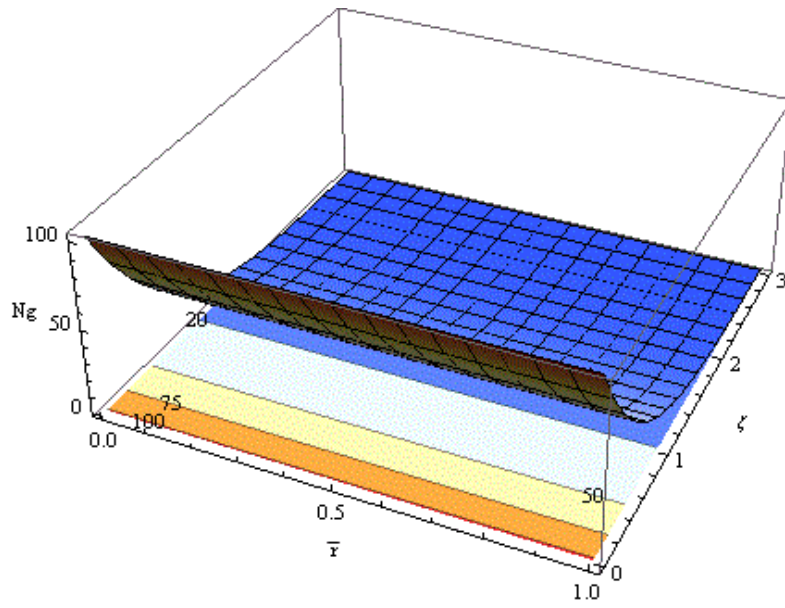
First Order



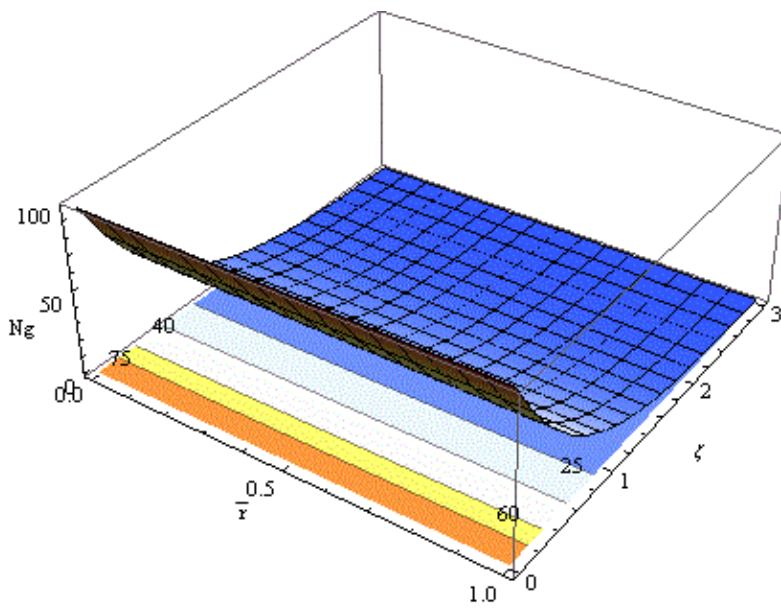
Second Order

Figure 5.14 : Variation of N_g with respect to \bar{r} and ζ in Neutral case ($W=0$)

Upper sides of Fig. 5.14-5.16 show the local entropy generation rate with only first order velocity slip and temperature jump boundary conditions and lower side of Fig. 5.14-5.16 show the local entropy generation rate with second order velocity slip and temperature jump boundary conditions.



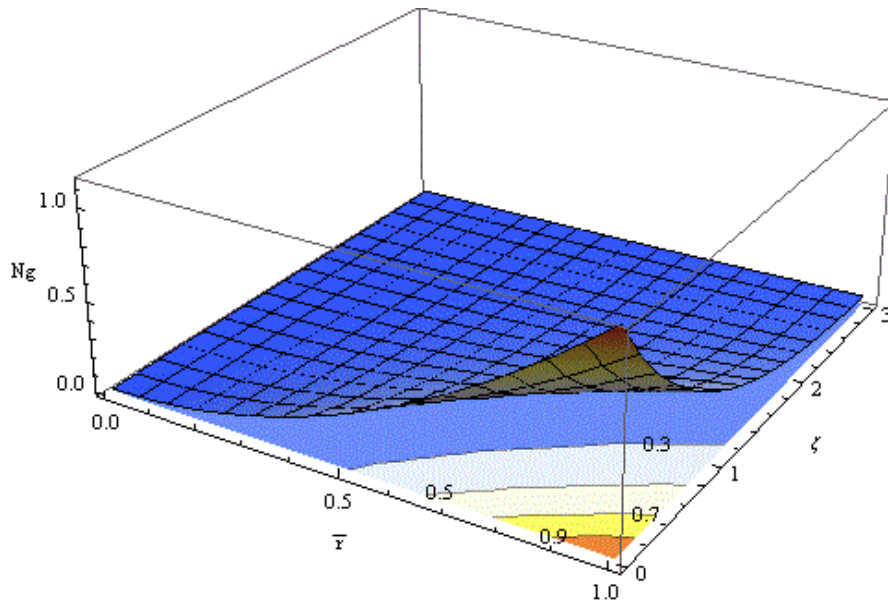
First Order



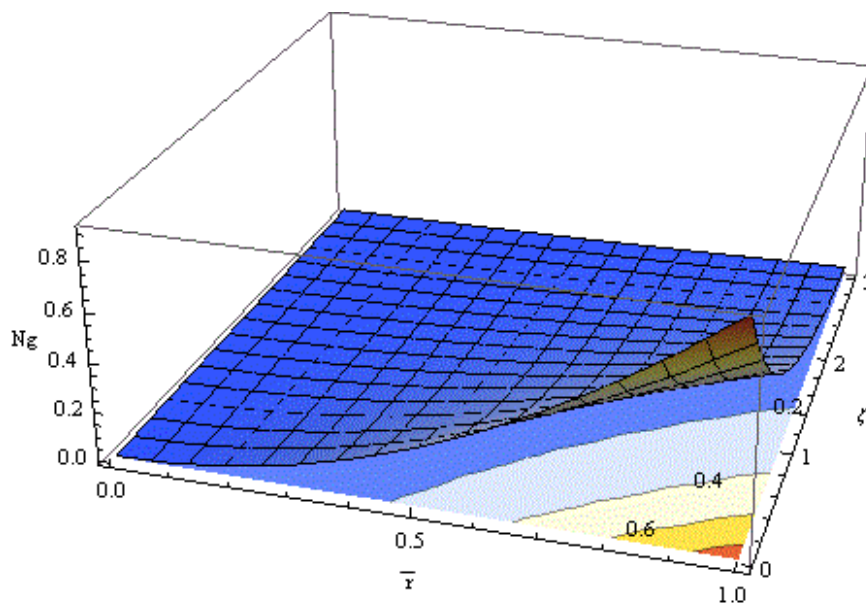
Second Order

Figure 5.15 : Variation of N_g with respect to \bar{r} and ζ in Suction case ($W=-1$)

Maximum local entropy generation rate occurs in suction case. It is observed that using second order velocity slip and temperature jump boundary decrease the local entropy generation rate.



First Order



Second Order

Figure 5.16 : Variation of N_g with respect to \bar{r} and ζ in Blowing case ($W=1$)

In blowing case, local entropy generation rate is very little. Local entropy generation rate occurs only the area while dimensionless disk radius closes to 1. On the remain area local entropy generation rate can be ignore.

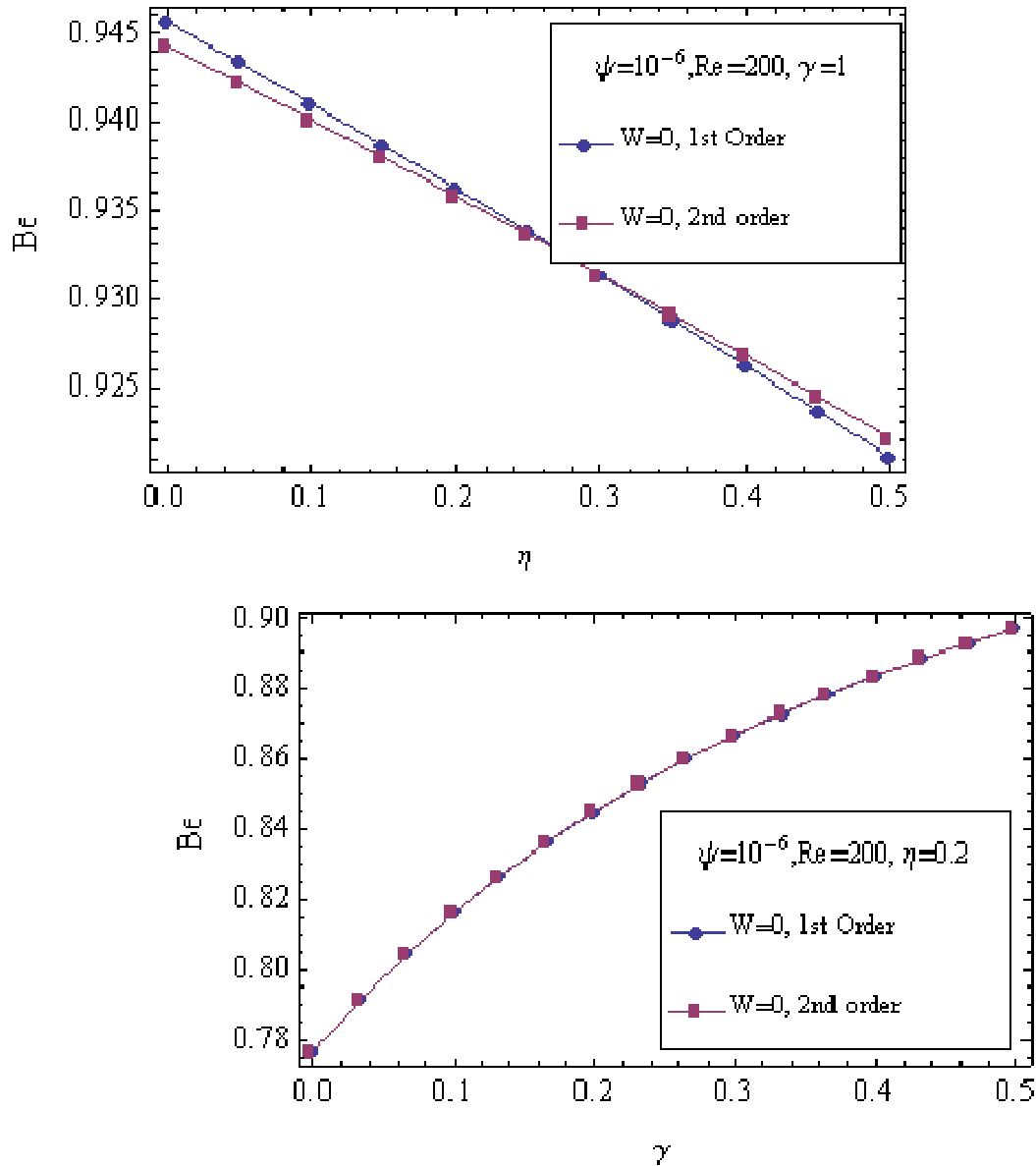


Figure 5.17 : Variation of Be with respect to slip factor and jump factor ($\bar{\tau}=1$) in Neutral case ($W=0$)

Fig. 5.17-5.19 show the mutual effects of different flow field conditions ($W=0$, $W=1$, $W=-1$) and first and second order boundary conditions. For neutral cases, $W=0$, Bejan number is not effected either the boundary condition first or second order. For the blowing case, $W=1$, Bejan number takes its possible smallest value since the entropy generation created by viscous effect dominates on total entropy generation. In the suction case, $W=-1$, Bejan number approaches to 1 since heat transfer entropy generation dominates on total entropy generation.

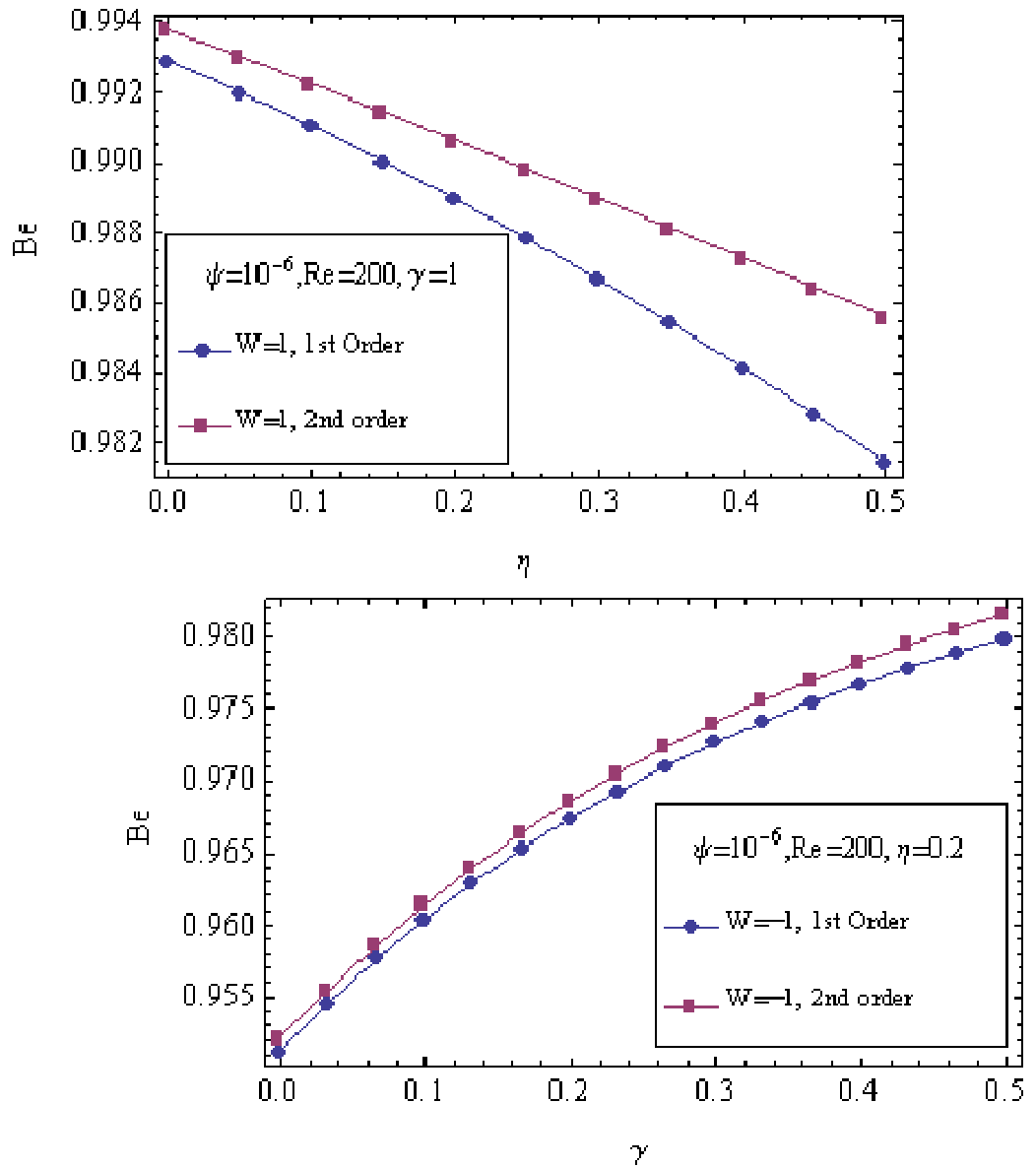


Figure 5.18 : Variation of Be with respect to slip factor and jump factor ($\bar{\tau}=1$) in Suction case ($W=-1$)

While the slip factor takes greater values, Bejan number increases. On the other hand, while the jump factor takes greater values, Bejan number reduces. The rarefaction effects reduce the velocity and temperature gradient so the entropy generation rate is decreases.

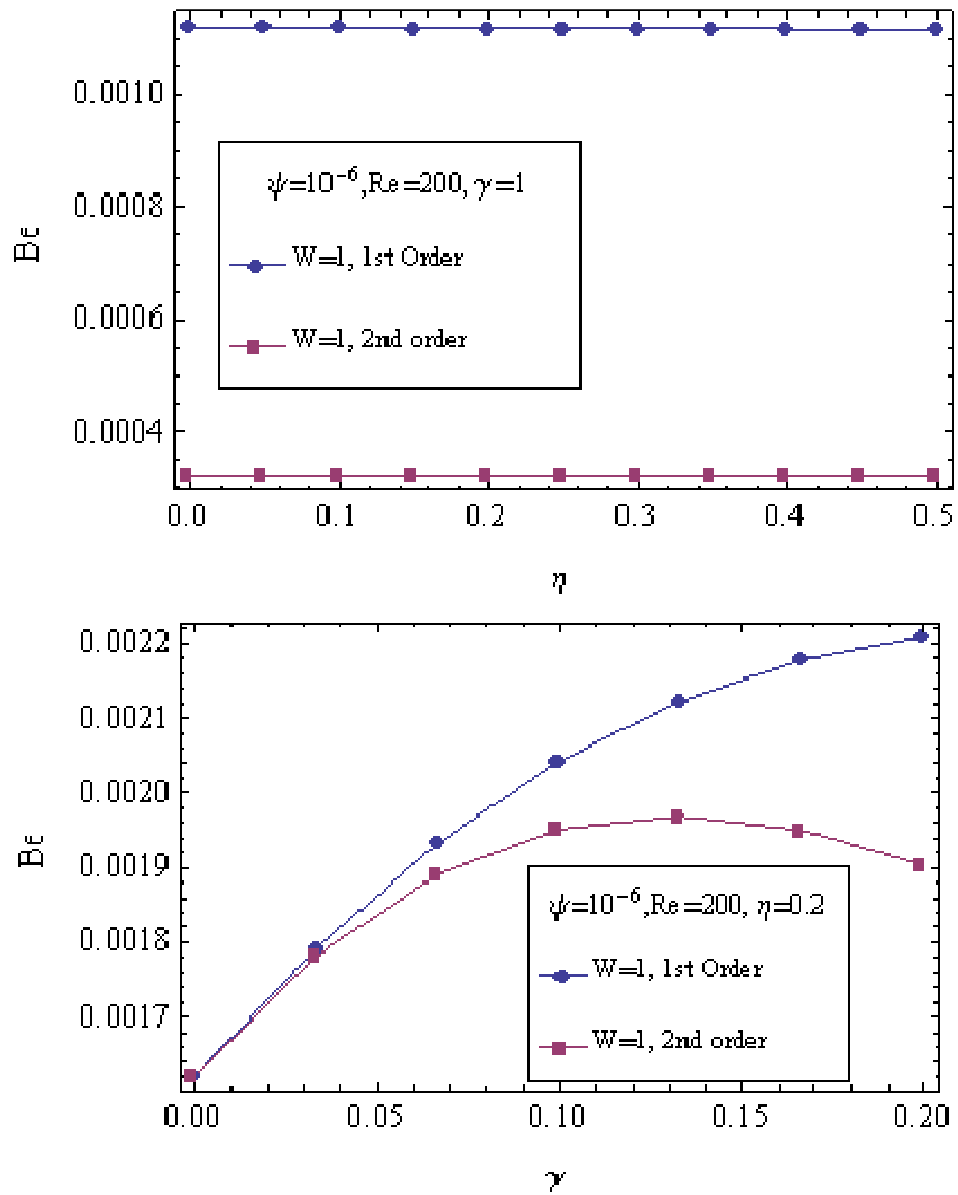
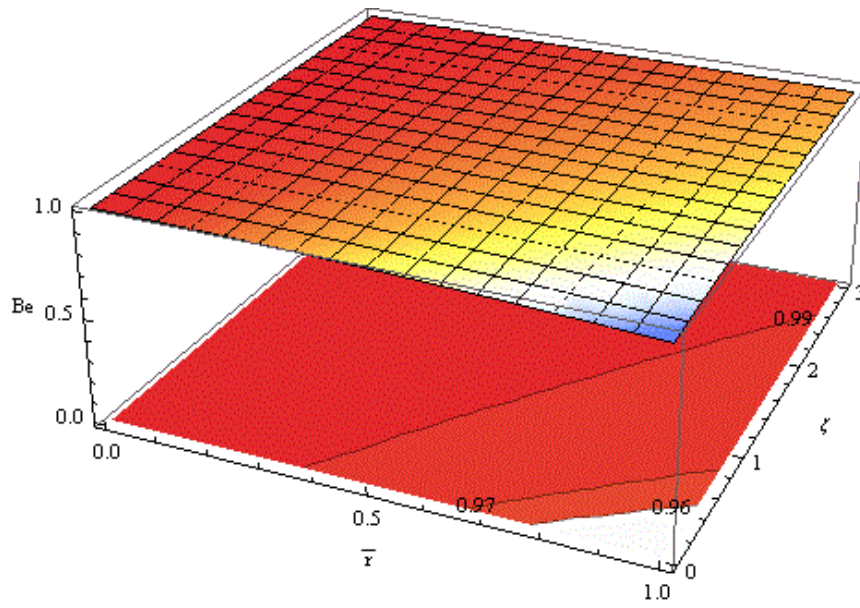
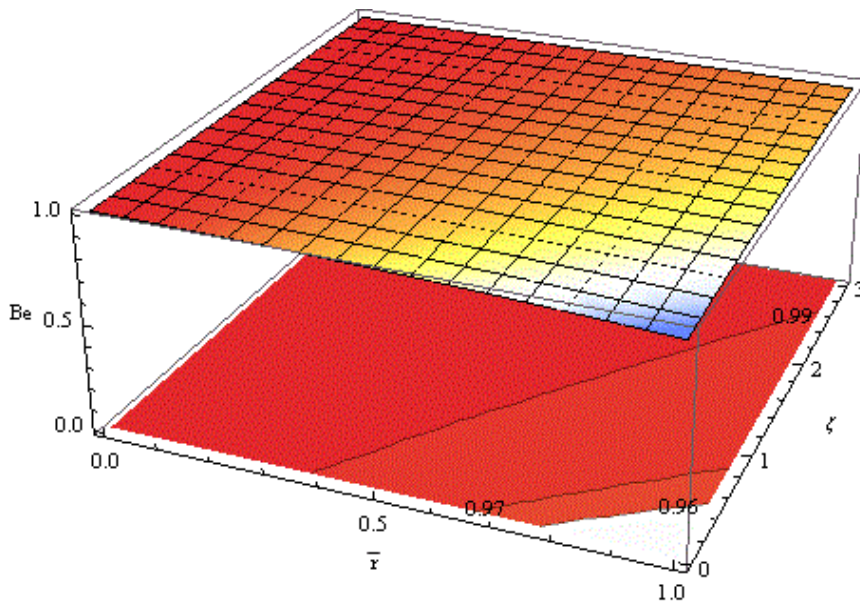


Figure 5.19 : Variation of Be with respect to slip factor and jump factor ($\bar{r}=1$) in Blowing case ($W=1$)

Be number is plotted as in Fig. 5.20-5.22. In neutral and suction cases, variations between Bejan numbers, which are determined by using first and second order velocity slip and temperature jump boundary condition, are ignorable. In blowing case, second order effects become admirable.



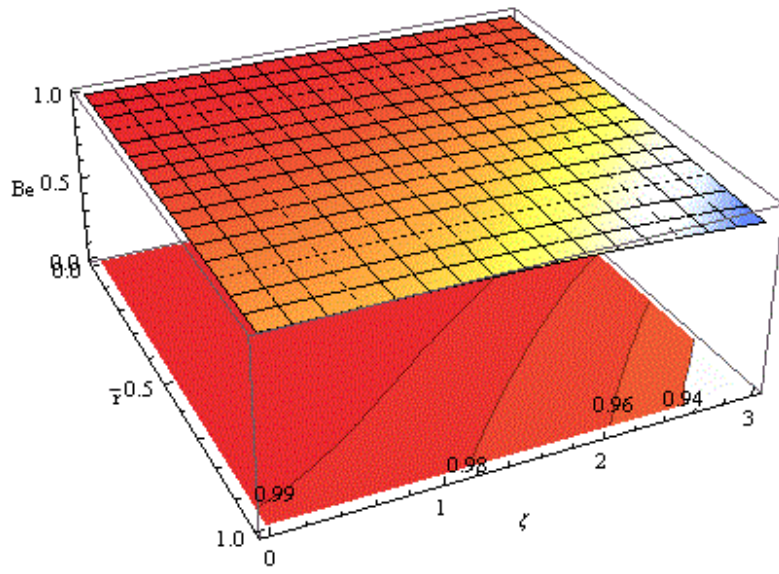
First Order



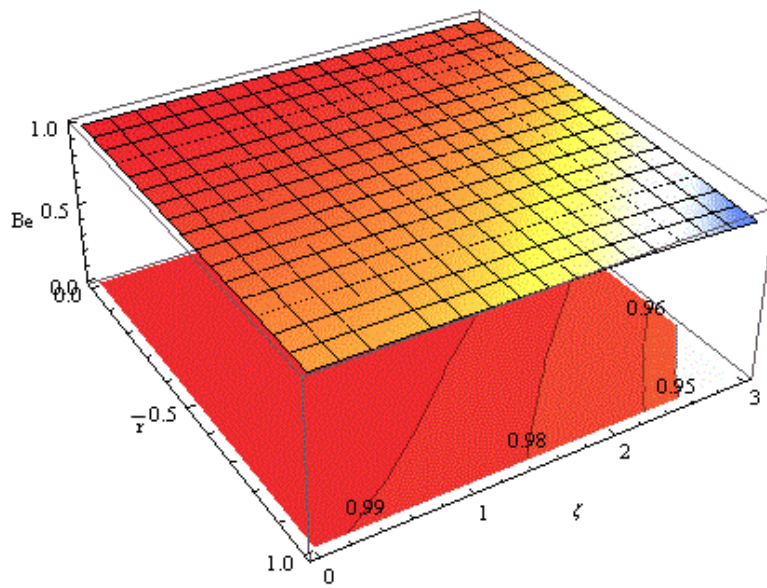
Second Order

Figure 5.20 : Variation of Be with respect to \bar{r} and ζ in Neutral case ($W=0$)

In neutral and suction case, heat transfer irreversibility is dominant. In blowing case, fluid friction is dominant excluded the area while the dimensionless disk radius close to 1.

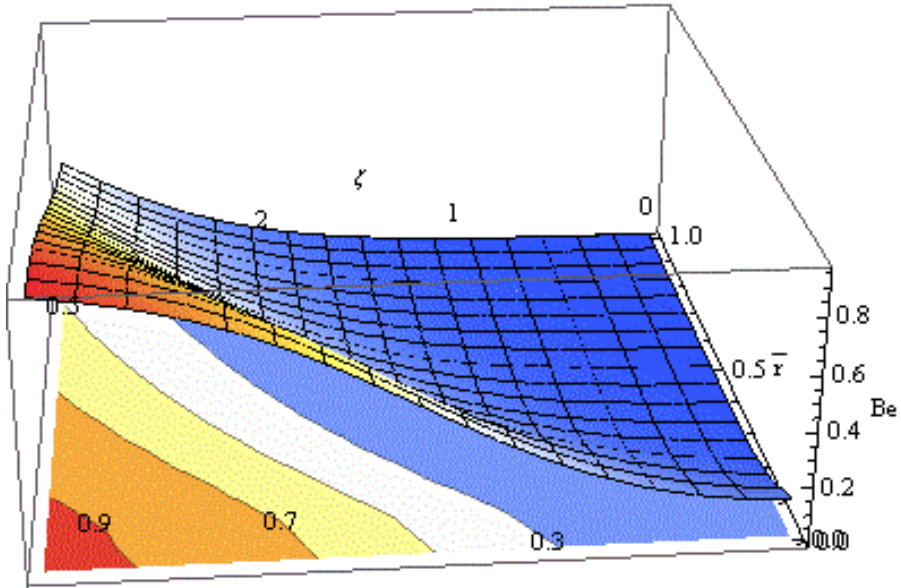


First Order

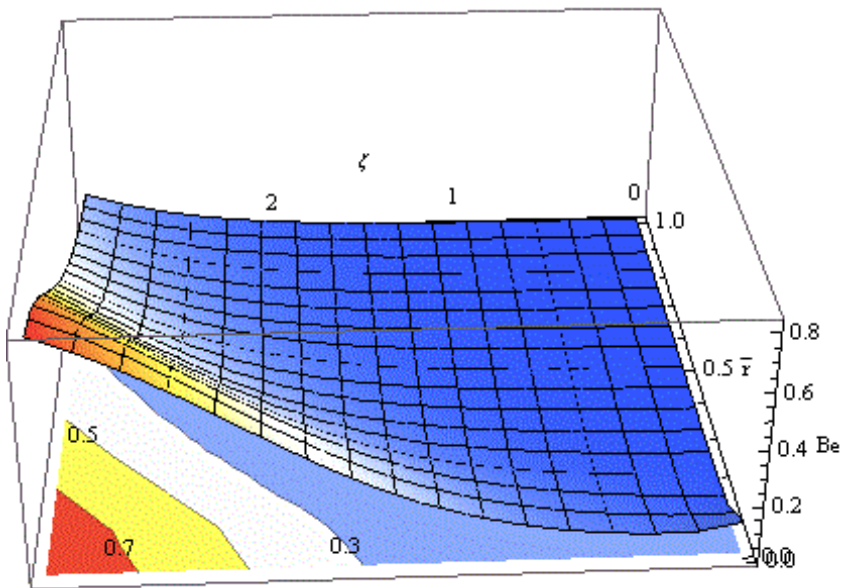


Second Order

Figure 5.21 : Variation of Be with respect to \bar{r} and ζ in Suction case ($W=-1$)



First Order



Second Order

Figure 5.22 : Variation of Be with respect to \bar{r} and ζ in Blowing case ($W=1$)

6. CONCLUSION

The paramount importance of this study is the application of the second order velocity slip and temperature jump boundary conditions, to a rotating free disk, for steady and axially symmetrical case in a Newtonian Fluid. Effect of second order boundary conditions on entropy generation is examined.

Additionally, these effects are examined in three different cases that are the suction, blowing and neutral cases. These types of flow field cases are frequently encountered in many engineering applications.

Navier-Stokes and energy equations with second order velocity slip and temperature jump boundary conditions are solved by using DTM and numerical integration.

Local and volumetric entropy generation and Bejan number are graphically presented for neutral, suction and blowing cases.

First and second order slip and jump boundary conditions were applied separately to show their sole effects. The common argument observed in these graphical representations is that the effect of slip factor and jump factor reduces the magnitude of entropy generation.

Using second order velocity slip and temperature jump boundary conditions decreases the entropy generation. This means that minimum the entropy generation maximum the available work. In other words, the efficiency of the system increases.

Finally one notices that to use the second order boundary conditions creates a difference in the total entropy generation, i.e., reducing the total entropy generation, which directly affects the efficiency calculation of the thermal system. That is vital for the design calculation of the energy consumptions.

REFERENCES

- [1] **Karman, T.**, 1921. *Über Laminare und Turbulente Reibung*. Z. Angew. Math.Mech., 1, 233-252.
- [2] **Cochran, W.G.**, 1934. *The flow due to a rotating disk*, Proc. Camb. Philos. Soc. 30 (3) , 365–375.
- [3] **Attia, H.A.**, 2009. *Steady Flow over a Rotating Disk in Porous Medium with Heat Transfer*, Nonlinear Analysis: Modelling and Control, Vol. 14, No. 1, 21–26.
- [4] **Andersson, H. and Rousselet M.**, 2005. *Slip flow over a lubricated rotating disk*, International Journal of Heat and Fluid Flow 27 , 329–335
- [5] **Osalusi, E., Side, J. and Harris, R.**, 2007. *The effects of Ohmic heating and viscous dissipation on unsteady MHD and slip flow over a porous rotating disk with variable properties in the presence of Hall and ion-slip currents*, International Communications on Heat and Mass Transfer, Vol. 34, 1017-29.
- [6] **Osalusi, E., Side, J. and Harris, R.**, 2008. *Thermal-diffusion and diffusion-thermo effects on combined heat and mass transfer of a steady MHD convective and slip flow due to a rotating disk with viscous dissipation and Ohmic heating*, International Communications on Heat and Mass Transfer, Vol. 35, 908-915.
- [7] **Jiji, M., J. and Ganatos P.**, 2010. *Microscale flow and heat transfer between rotating disks*, International Journal of Heat and Fluid Flow 31, 702–710
- [8] **Turkyilmazoglu M.**, 2011. *Exact solutions for the incompressible viscous magnetohydrodynamic fluid of a rotating disk flow*, International Journal of Non-Linear Mechanics 4, 306–311
- [9] **Arikoglu, A., Komurgoz G. and Ozkol, I.**, 2008. *Effect of slip on the entropy generation from a single rotating disk*, Journal of Fluids Engineering-Transactions of the ASME, 130(10), 101202.
- [10] **Hooman, K., Hooman, F., Famouri, M.**, 2009. *Scaling effects for flow in micro-channels: Variable property, viscous heating, velocity slip, and temperature jump*, International Communications in Heat and Mass Transfer, 36, 192–196.
- [11] **Karniadakis, G.E., Beskok, A.**, 2002. *Microflows: Fundamentals and Simulation*, Springer-Verlag, New York, 56.
- [12] **Aziz A.**, 2010. *Hydrodynamic and thermal slip flow boundary layers over a flat plate with constant heat flux boundary condition*, Commun Nonlinear Sci Numer Simulat, 15, 573-580

- [13] **Arikoglu A., Komurgoz G., Ozkol I., and Gunes A.Y.**, 2010. *Combined Effects of Temperature and Velocity Jump on the Heat Transfer, Fluid Flow, and Entropy Generation Over a Single Rotating Disk*, J. Heat Transfer 132, 111703
- [14] **Renksizbulut, M., Niazmand H. and Tercan, G.**, 2006. *Slip-flow and heat transfer in rectangular microchannels with constant wall temperature*, International Journal of Thermal Sciences, 45, 870–881.
- [15] **Xiao, N., Elsnab, J., Ameal, T.**, 2009, “Microtube gas flows with second-order slip flow and temperature jump boundary conditions”, International Journal of Thermal Sciences, 48, pp.243–251.
- [16] **Meolans, J.G.**, 2003. *Thermal slip boundary conditions in vibrational nonequilibrium flows*, Mechanics Research Communications 30, 629–637.
- [17] **Beskok A., Karniadakis G. and Trimmer W.**, 1996. *Rarefaction and Compressibility Effects in Gas Microflows*, J. Fluids Eng. 118, 448, DOI:10.1115/1.2817779
- [18] **Deissler R.**, 1964. *An analysis of second-order slip flow and temperature jump boundary conditions for rarefied gases*, Int. J. Heat Mass Trans. 7, 681–694.
- [19] **Hamdan M. A., Al-Nimr M. A. and Hammoudeh**, 2010. *Effect of Second Order Velocity-Slip/Temperature-Jump on Basic Gaseous Fluctuating Micro-Flows*, J. Fluids Eng. 132, 074503 , DOI:10.1115/1.4001970
- [20] **Haddad, O., Al-Nimr, M., and Abuzaid, M.**, 2005. *The Effect of Frequency of Fluctuating Driving Force on Basic Gaseous Micro-Flows*, Acta Mech., 179, 249–259.
- [21] **Hoomann, K.**, 2007. *Entropy generation for microscale forced convection: Effects of different thermal boundary conditions, velocity slip, temperature jump, viscous dissipation, and duct geometry*, International Communications in Heat and Mass Transfer, 34, 945–957.
- [22] **Niazmand H. and Rahimi B.**, 2010. *High Order Slip and Thermal Creep Effects in Micro Channel Natural Convection*, ASME Conf. Proc. 2010, 705, DOI:10.1115/ FEDSM-ICNMM2010-30688
- [23] **Zahmatkesh I., Alishahi M. and Emdad H.**, 2011. *New velocity-slip and temperature-jump boundary conditions for Navier–Stoke computation of gas mixture flows in microgeometries*, Mechanics Research Communications 38,417– 424
- [24] **Zhou, J.K.**, 1986. *Differential Transformation and its Application for Electrical Circuit*, Huazhong University Press, Wuhan, China

- [25] **Mao, Q.**, 2012. *Design of piezoelectric modal sensor for non-uniform Euler-Bernoulli beams with rectangular cross-section by using differential transformation method*”, Mechanical Systems And Signal Processing 33 pp.142-154
- [26] **Rahimi,M., Hosseini,M.J., Barari, A., Domairry, G.**, 2011. *Differential Transformation Method for Temperature Distribution in a Radiating Fin*, Heat Transfer Resources, 42, 403-414
- [27] **Arikoglu A. and Ozkol, I.**, 2006. *Solution of differential-difference equations by using differential transform method*, Applied Mathematics and Computation 181,153-162
- [28] **Arikoglu A. and Ozkol, I.**, 2006. *On the MHD and slip flow over a rotating disk with heat transfer*, International Journal of Numerical Methods for Heat & Fluid Flow 16(2), 172–184.
- [29] **Benton, E.R.**, 1966. *On the flow due to a rotating disk*, J. Fluid Mech. 24, 781–800.
- [30] **Schaaf SA and Chambre PL** ,1961. *Flow of rarefied gases*, Princeton University Press, Princeton
- [31] **Korzhova, V. N.**, 2009, *Motion Analysis of Fluid Flow in a Spinning Disk Reactor*, Graduate School Theses and Dissertations.
- [32] **Bejan, A.**, 1980. *Second law analysis in heat transfer*, Energy-The International Journal 5, 721-732.
- [33] **Zhang W., Meng Z., Wei X.**, 2012. *A review on slip models for gas microflows*, Microfluidics and Nanofluidics, Volume 13, Issue 6, 845-882

CURRICULUM VITA



Candidate's full name: Ahmet Yaşar Güneş

Place and date of birth: Ordu 14/07/1982

Permanent Address: Başakşehir 5.Etap 1.Kısım Salacak Sitesi A9 blok D:31
Başakşehir/İstanbul

**Universities and
Colleges attended:** İstanbul Technical University

Ordu Anatolian High School

Publications:

- Arikoglu A.,Komurgoz G., Ozkol I., and Gunes A.Y., 2010, “Combined Effects of Temperature and Velocity Jump on the Heat Transfer, Fluid Flow, and Entropy Generation Over a Single Rotating Disk ” J. Heat Transfer 132, pp.111703
- Arikoglu A.,Komurgoz G., Ozkol I., and Gunes A.Y., 2010, “Investigations of Heat Transfer over a Rotating Disk in case of Temperature and Velocity Jump Conditions by using DTM” ASME 2010 10th Biennial Conference on Engineering Systems Design and Analysis ESDA2010-25042 pp. 687-693